Arabian Journal of Chemistry (2022) **15**, 104009

King Saud University

Arabian Journal of Chemistry

www.ksu.edu.sa
www.sciencedirect.com

ORIGINAL ARTICLE

Coordination complexes of rare earth metals with hydrazine and isomeric acetamidobenzoates as ligands– spectral, thermal and kinetic studies

Helen Pricilla Bai Esudass [a], **Vairam Sundararajan** [c,*], **Dinesh Kirupha Selvaraj** [b]

[a] *Department of Chemistry, Park College of Engineering and Technology, Coimbatore 641659, Tamil Nadu, India*
[b] *Department of Environmental Engineering, Park College of Technology, Coimbatore 641659, Tamil Nadu, India*
[c] *Department of Chemistry, Government College of Technology, Coimbatore 641 013, Tamil Nadu, India*

Received 22 February 2022; accepted 23 May 2022
Available online 6 June 2022

KEYWORDS

Acetamidobenzoic acid;
SEM-EDAX;
Lanthanides;
TG–DTA;
Magnetic susceptibility

Abstract The isomeric acetamido benzoic acids (abbreviated as acambH) on reaction with hydrazine hydrate and lanthanides, La^{3+}, Ce^{3+}, Pr^{3+}, Nd^{3+}, Sm^{3+} and Gd^{3+} form complexes of formulae, $[Ln\{x\text{-}C_6H_4(CH_3CONH)\}_3(N_2H_4)]$ where x = 2 (or) 3 (or) 4, at pH 3–4.5 in (1:1) aqueous ethanolic medium, which are insoluble in water and organic solvents. They are characterized by using elemental analysis, IR, UV, ^{13}C, ^{1}H NMR and mass spectroscopic, XRD, SEM-EDAX, thermal and conductance studies. The difference between IR bands of $\nu_{C=O\ asym}$ (acid) and $\nu_{C=O\ sym}$(acid) range, 122–166 cm^{-1} supports the bidental coordination of carboxylate ions to metal. $\nu_{N\text{-}N}$ values of 955 to 980 cm^{-1}, substantiate bridging bidentate coordination of hydrazine to metal. $\nu_{C=O}$ of amide group 1632 to1709 cm^{-1} indicates its non-coordination with metal. The thermal studies reveal that complexes undergo dehydrazination between 52 and 180 °C and exothermic degradation into phthalate intermediate between 172 and 496 °C and further degradation to form microsized metal oxide around 600 °C. The magnetic susceptibility measurements indicated that the presence of metals in the same electronic state and electronic spectral assignments suggested that the coordination number is eight for the complexes. The conductance measurement results in DMSO medium indicated that the complexes are neutral. The ^{13}C – NMR, ^{1}H- NMR and the LC-Mass techniques substantiated the composition of the complexes.

* Corresponding author.
E-mail address: drsvairam@rediffmail.com (V. Sundararajan).
Peer review under responsibility of King Saud University.

Production and hosting by Elsevier

https://doi.org/10.1016/j.arabjc.2022.104009
1878-5352 © 2022 Published by Elsevier B.V. on behalf of King Saud University.

1. Introduction

Hydrazine, a versatile ligand with two basic sites, forms a variety of complexes with alkaline earth metals and with lanthanides and actinides (Schmidt et al., 1984). While studying these hydrazine complexes and their derivatives, more attention is given on their thermal behaviour. The thermal Chemistry of these complexes is more attractive since hydrazine is an exothermic compound and an enormous amount of heat energy is liberated due to the formation of nitrogen molecule, making metal oxide residues nanosized. Hence the metal complexes containing hydrazine have been utilized and are being exploited as precursors to metal oxides and mixed metal oxides such as ferrites, cobaltites, etc., (Ravindranathan and Patil, 1986, Ravindranathan et al., 1987) by their low temperature decomposition. Many complexes of inner transition metals with hydrazine and aliphatic and aromatic carboxylic acids have been explored (Govindarajan et al., 1986, Kuppusamy et al., 1996; Vairam and Govindarajan, 2006; Sivasankar et al., 2004, Bai and Vairam, 2013; Devipriya et al., 2013; Parimalagandhi and Vairam, 2014; Parimalagandhi et al., 2016). The transition metal complexes with acetamido substituted benzoic acids are also found in the literature (Mascarenhas et al., 1980; Li et al., 2007; Yang et al., 2009; Yang et al., 2009a; Manin et al., 2014; Manin et al., 2014a; Manin et al., 2014b; Almeida et al., 2015; Rakse et al., 2021). Additional- reports of 4-acambH lanthanides (Man, 2010; Yin et al., 2011; Wang et al., 2009; Gupta, 2019; TanTong et al., 2018) such as synthesis, crystal structures and photoluminescence of lanthanide coordination polymers with 4-acambH, coordination behavior of radii-dependent lanthanides with 4-acambH and 1, 10-phenanthroline, microbial neuraminidase inhibitors of derivatives of substituted 4-acambH, metallo-supramolecular Ti-based M_4L_4 cage assembly of 4-acambH are also available in the literature. Helen et al. has reported the synthesis, characterization and thermal degradation of transition metal complexes of isomeric acetamido benzoic acids (Bai and Vairam, 2013; Bai and Vairam, 2020). In this paper, synthesis, spectral and thermal studies of some lanthanide complexes of 2-acetamido, 3-acetamido and 4-acetamido benzoic acids (Fig. 1) with hydrazine are presented for the first time. Similarly self-assembled molecular structures of organic compounds and Recent advances in hybrid organic–inorganic materials with spatial architecture for state-of-the-art applications are carried out (Zoubi, et al., 2021; Zoubi, et al., 2020).

2. Experimental

2.1. Preparation of $[Ln\{2/3/4\text{-}C_6H_4(NHCOCH_3)_3\}.(N_2H_4)]$, where Ln = La, Ce, Pr, Nd, Sm& Gd

Lanthanum oxide (0.325 g, 1 mmol) was dissolved in a minimum quantity of 1:1 nitric acid (HNO_3 Sp. gravity 1.42 g/mL), evaporated to eliminate excess of acid, and the residue was dissolved in 20 mL of ethanol. To a freshly prepared (1:1) ethanolic solution (40 mL) of the ligands containing 2-acetamido benzoic acid (1.075g, 6 mmol): hydrazine hydrate (0.912g, 8 mmol), the alcoholic solution of the metal was added stirring the reaction mixture vigorously. A pale yellow microcrystalline solid formed immediately at pH 3 and was kept over a hot water bath for 5 min at 90 °C. The product was cooled, filtered, and washed with ethanol and ether and then dried in a desiccator.

All the other complexes of 2, 3 & 4-acetamido benzoates were prepared by a similar procedure by adding the respective metal nitrate solution to the ligand solution in the mole ratios Metal:Acid:Base ≡ 1:6:8, 1:4:4 and 1:6:8 at pH 3, 4.5 respectively. The microcrystalline solid products formed were filtered, washed with alcohol and ether, and then they were dried over anhydrous $CaCl_2$ in desiccators. The preparation scheme is described below.

$$\begin{aligned} &Et.\left[\mathrm{Ln(NO_3)_3}\right] + \{Et.[\mathrm{N_2H_4.H_2O} + x - \mathrm{acmbH}]\} \\ &\xrightarrow{pH(3-4.5)} \text{Pale yellow microcrystalline complex} \\ &Et. - \text{Aqueous ethanolic solution \&} \\ &x = 2\ (\text{or})\ 3\ (\text{or})\ 4 - \text{acetamidobenzoic acid} \end{aligned} \quad (1)$$

2.2. Physicochemical methods

The hydrazine content in all complexes was determined volumetrically using 0.025 M Potassium iodate solution under Andrews' conditions (Vogel, 2019). The metal content was determined by EDTA complexometric titration (Vogel, 2019) after decomposing a known weight of the sample with 1:1 HNO_3. Magnetic susceptibility measurements of the complexes were carried out on a vibrating sample magnetometer, VSM EG & G model 155. The electronic spectra for solid-state complexes were obtained using a varian, Cary 5000 recording spectrophotometer. Infra-red spectra were recorded using KBR disc (4000–400 cm^{-1}) on a Shimadzu FTIR-8201 (PC) S spectrophotometer. The simultaneous TG-DTA studies were done on a Perkin Elmer, Diamond TG/DTA analyzer and the curves were obtained in static air using 5–10 mg of the samples at the heating rate of 10 °C/min. The XRD patterns were recorded on a Bruker AXS D8 Advance diffractometer with an X-ray source Cu, wavelength 1.5406 Å using a Si (Li) PSD detector. The elemental analysis was carried out using a CHNS Elementar Vario EL- III Elemental Analyzer. The mass spectrum was obtained using TQD–WATERS

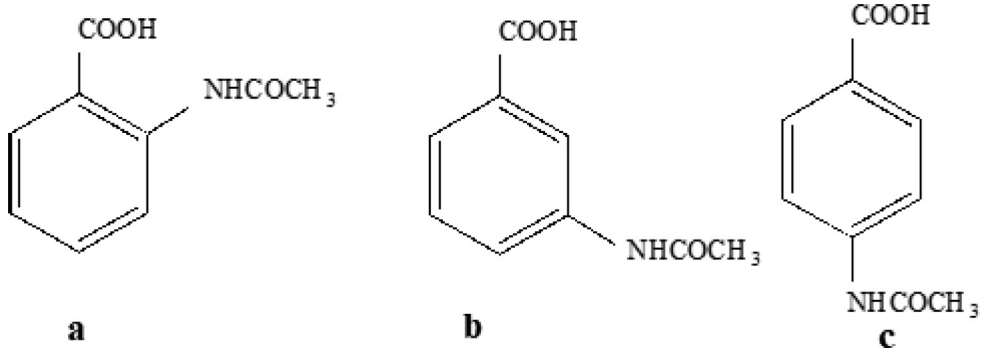

Fig. 1 (a-c): Chemical structure of Ligands employed; 1(a): 2-acetamido benzoic acid (2-acambH); 1(b): 3-acetamido benzoic acid (3-acambH); 1(c): 4-acetamido benzoic acid (4-acambH).

Table 1 Magnetic Susceptibility data of lanthanide complexes of isomeric acetamido benzoic acid and hydrazine.

M^{3+} ion	$4f^n$	S	L	J	μ_{eff} (Anal.(Calcd.)) BM		
					$[Ln(2\text{-acamb})_3(N_2H_4)]$	$[Ln(3\text{-acamb})_3(N_2H_4)]$	$[Ln(4\text{-acamb})_3(N_2H_4)]$
La	0	0	0	0	–	–	–
Ce	1	ø	3	5/2	2.5(2.54)	2.3(2.41)	2.4(2.48)
Pr	2	1	5	4	3.3(3.48)	3.2(3.51)	3.3(3.46)
Nd	3	3/2	6	9/2	3.6 (3.71)	3.4 (3.63)	3.5 (3.58)
Sm	5	5/2	5	5/2	1.6(0.98)	1.4(0.88)	1.5(0.94)
Gd	7	7/2	0	7/2	8.1(7.92)	8.0(7.78)	8.3(7.94)

liquid chromatography coupled mass spectrophotometer. The ^{13}C and ^{1}H NMR spectras were recorded for all the samples dissolved in DMSO using JEOL-NMR device with an operating frequency of 600 MHZ.

3. Results and discussion

All the complexes are insoluble in organic solvents like ethanol and ether. They are soluble in DMSO and sparingly soluble in water.

3.1. Magnetic susceptibility and electronic spectra measurements

The effective magnetic moment values of La, Ce, Pr, Nd, Sm, and Gd complexes were obtained from the VSM graph using the following formula $\mu_{eff} = 2.828 \sqrt{\chi_m T}$), where χ_m (magnetic moment of the lanthanide samples) = (Molecular Weight of the Sample / Sample Wt) X Slope (Bohr Magneton) and tabulated (Table 1), which are in good agreement with reported values (Want and Shah, 2016). Besides the observed values were compared with theoretical effective values calculated using the formula $\mu_{eff} = gJ \sqrt{J(J+1)}\ \mu B$, where μ_B - BM respectively.

The absorptions observed in electronic spectra of Pr and Nd complexes and the levels assigned are given in Table 2. The absorptions of Nd complex are comparable to that of Nd bis-bipyridyl complexes suggesting coordination number 8 in it (Petit et al., 2006).

On comparison of electronic spectral data of Pr and Nd complexes with their aquo complexes (Parimalagandhi et al., 2016), the shifts in band positions are observed compared to those of aquo lanthanide metal ions. It is observed in case of neodymium complexes, there is decrease in the wave number by 346–1757 cm^{-1}, from its aquo complex, whereas there is no considerable change in wave number of praseodymium complex from its aquo complex. This shift, a measure of metal–ligand interaction, has been ascribed to nephelauxeatic effect (Jung et al., 2017). The involvement of f-orbital in M—O bonding is an important component of covalency (Berryman et al., 2019).

The Sinha's covalency parameter (δ %) was calculated using the expression (Eq. (1)),

$$\delta = \frac{(1-\beta)}{\beta} \times 100 \quad (1)$$

where $\beta = (1/n)\sum (v^i_{complex}/v^i_{aquo})$; β is the average value of the ratio $v_{complex}$ / v_{aquo} and n is the number of transitions considered. The values of δ either positive (covalent bonding) or negative (ionic bonding). Moreover, the Sinha's covalency parameter (Petit et al., 2006) observed here indicates that Nd ion of 2, 3 and 4 isomeric acids exhibit higher covalency (3.76–47.2) than that of Pr ion which implies that the Nd complexes exhibit covalent nature. The lower δ values (−0.3 to 0.2) of praseodymium ion of the complexes of same isomeric acetamido benzoic acids indicate that they are ionic.

3.2. IR spectra of complexes

The analytical data and absorption frequencies of complexes are shown in Table 3 and the infrared spectra of all compounds are given in Figs. 2–4.

Table 2 Electronic Spectroscopic data of lanthanide complexes of isomeric acetamido benzoic acids and hydrazine.

Complexes	Observed bands (cm^{-1})	Assigned Levels	Parameters
$[Nd(2\text{-}C_6H_4(CH_3CONH)COO\}_3.(N_2H_4)]$	17007, 12,407 & 11,025	$^2G_{7/2}$, $^4F_{5/2}$& $^4F_{3/2}$	β = 1.0170 % δ = -1.671
$[Nd(3\text{-}C_6H_4(CH_3CONH)COO\}_3.(N_2H_4)]$	25840, 17182, 13,459 & 12,392	$^2P_{3/2}$, $^2G_{7/2}$, $^4F_{7/2}$& $^4F_{5/2}$	β = 0.9974 % δ = 0.2606
$[Nd(4\text{-}C_6H_4(CH_3CONH)COO\}_3.(N_2H_4)]$	26109, 17637, 16807, 13,578 & 12,403	$^2P_{3/2}$, $^2G_{7/2}$, $^4G_{5/2}$, $^4F_{7/2}$& $^4F_{5/2}$	β = 0.9974 % δ = 0.2606
$[Pr(2\text{-}C_6H_4(CH_3CONH)COO\}_3.(N_2H_4)]$	22371, 20,704 & 11,038	$^3P_2$, $^3P_0$&$^1G_4$	β = 0.9987 % δ = 0.1301
$[Pr(3\text{-}C_6H_4(CH_3CONH)COO\}_3.(N_2H_4)]$	22,422 & 21,186	$^3P_2$&$^1I_6$	β = 0.9829 % δ = 1.739
$[Pr(4\text{-}C_6H_4(CH_3CONH)COO\}_3.(N_2H_4)]$	22487, 21368, 20747& 16,798	$^3P_2$,$^1I_6$, $^3P_0$&$^1D_2$	β = 0.9816 % δ = 1.8744

Table 3 Analytical and IR data of lanthanide complexes of isomeric acetamido benzoic acids and hydrazine.

Complexes	Analytical data					IR data (cm^{-1}) b- broad; s-sharp; m-medium;					
	Carbon	Hydrogen	Nitrogen	Hydrazine	Metal	$\nu_{C=O}$ asym	$\nu_{C=O}$sym	$\nu_{N\text{-}N}$	ν_{OH}	$\nu_{N\text{-}H}$	$\nu_{C=O(amido\ gp)}$
	Anal.(Calcd.)	Anal.(Calcd.)	Anal.(Calcd.)	Anal.(Calcd.)	Anal.(Calcd.)						
2-acetamido benzoate lanthanides[Ln(2-acamb)$_3$(N_2H_4)] where Ln = La, Ce, pr, Nd, Sm and Gd											
[La{2-C_6H_4(CH_3CONH)COO}$_3$(N_2H_4)]	45.90(45.93)	3.92(4.00)	9.73 (9.92)	4.49(4.54)	19.43(19.69)	1580b	1439 s	959 s	3385 b	3275 m	1674 s
[Ce{2-C_6H_4(CH_3CONH)COO}$_3$(N_2H_4)]	45.88(45.85)	3.78(3.99)	9.85(9.91)	4.50(4.53)	19.72(19.83)	1584 s	1439 s	955 s	3335 s	3275 m	1674 s
[Pr{2-C_6H_4(CH_3CONH)COO}$_3$ (N_2H_4)]	45.11(45.80)	3.78(3.99)	9.82(9.89)	4.53(4.52)	19.90(19.92)	1580 s	1441 s	961 s	3414 b	3150 m	1670 m
[Nd{2-C_6H_4(CH_3CONH)COO}$_3$(N_2H_4)]	45.43(45.58)	3.88(3.97)	9.91(9.85)	4.53(4.50)	19.87(20.29)	1584 s	1443 s	961 m	3389 b	3146 b	1676 m
[2-Sm{C_6H_4(CH_3CONH)COO}$_3$(N_2H_4)]	45.21(45.19)	3.79(3.94)	9.72(9.76)	4.54(4.46)	20.76 (20.97)	1583 m	1443 s	961 s	3431 b	3152 m	1676 s
[2-Gd{C_6H_4(CH_3CONH)COO}$_3$(N_2H_4)]	44.65(44.76)	3.93(3.90)	9.59(9.67)	4.36(4.42)	21.77 (21.73)	1593 s	1452 s	968 s	3360 s	3202b	1632 s
3-acetamido benzoate lanthanides [Ln(3- acamb)$_3$(N_2H_4)] where Ln = La, Ce, pr, Nd, Sm and Gd											
[La{3-C_6H_4(CH_3CONH)COO}$_3$(N_2H_4)]	45.72(45.93)	3.88(4.00)	9.89 (9.92)	4.41(4.54)	19.36(19.69)	1609 s	1489 s	980 s	3435 b	3337 m	1709 s
[Ce{3-C_6H_4(CH_3CONH)COO}$_3$(N_2H_4)]	45.79(45.85)	3.85(3.99)	9.76(9.91)	4.47(4.53)	19.80(19.83)	1555 m	1395 s	978 s	3416 m	3254 s	1655 s
[Pr{3-C_6H_4(CH_3CONH)COO}$_3$(N_2H_4)]	45.28(45.80)	3.84(3.99)	9.90(9.89)	4.43(4.52)	19.78(19.92)	1555 s	1393 s	978 s	3414 b	3252 m	1657 s
[Nd{3-C_6H_4(CH_3CONH)COO}$_3$(N_2H_4)]	45.02(45.58)	4.00(3.97)	9.80(9.85)	4.44(4.50)	20.00(20.29)	1553 m	1395 s	978 s	3416 b	3260 s	1659 s
[Sm{3-C_6H_4(CH_3CONH)COO}$_3$(N_2H_4)]	45.10(45.19)	3.87(3.94)	9.63(9.76)	4.41(4.46)	20.92(20.97)	1612 m	1485 s	980 s	3337 s	3273 b	1709 s
[Gd{3-C_6H_4(CH_3CONH)COO}$_3$(N_2H_4)]	44.38(44.76)	3.79(3.90)	9.59(9.67)	4.40(4.42)	21.67(21.73)	1559 m	1393 s	978 s	3431b	3202 m	1659 s
4-acetamido benzoate lanthanides [Ln(4acamb)$_3$(N_2H_4)] where Ln = La, Ce, pr, Nd, Sm and Gd											
[La{4-C_6H_4(CH_3CONH)COO}$_3$(N_2H_4)]	45.89 (45.93)	3.98(4.00)	9.90 (9.92)	4.56(4.52)	19.57(19.60)	1559b	1434 b	963 s	3313 b	3274	1675 b
[Ce{4-C_6H_4(CH_3CONH)COO}$_3$(N_2H_4)]	45.83(45.85)	4.00(3.99)	9.89(9.91)	4.53(4.51)	19.69(19.74)	1523 s	1401 s	966 s	3529 s	3302	1675 s
[Pr{4-C_6H_4(CH_3CONH)COO}$_3$(N_2H_4)]	45.78(45.80)	3.94(3.99)	9.90(9.89)	4.49(4.50)	19.85(19.83)	1553 s	1405 s	965 s	3309 s	3203	1674 s
[Nd{4-C_6H_4(CH_3CONH)COO}$_3$(N_2H_4)]	45.32(45.58)	4.02(3.97)	9.78(9.85)	4.45(4.48)	19.98(20.21)	1553 s	1403 s	965 s	3309 s	3206	1674 s
[Sm{4-C_6H_4(CH_3CONH)COO}$_3$(N_2H_4)]	45.32(45.19)	3.87(3.94)	9.63(9.76)	4.48(4.45)	20.87(20.89)	1556 s	1394 s	965 s	3304 s	3269	1675 s
[Gd{4-C_6H_4(CH_3CONH)COO}$_3$(N_2H_4)]	44.73(44.76)	3.85(3.90)	9.59(9.67)	4.39(4.40)	21.67(21.64)	1558 m	1414 s	966 s	3305 s	3271	1674 s

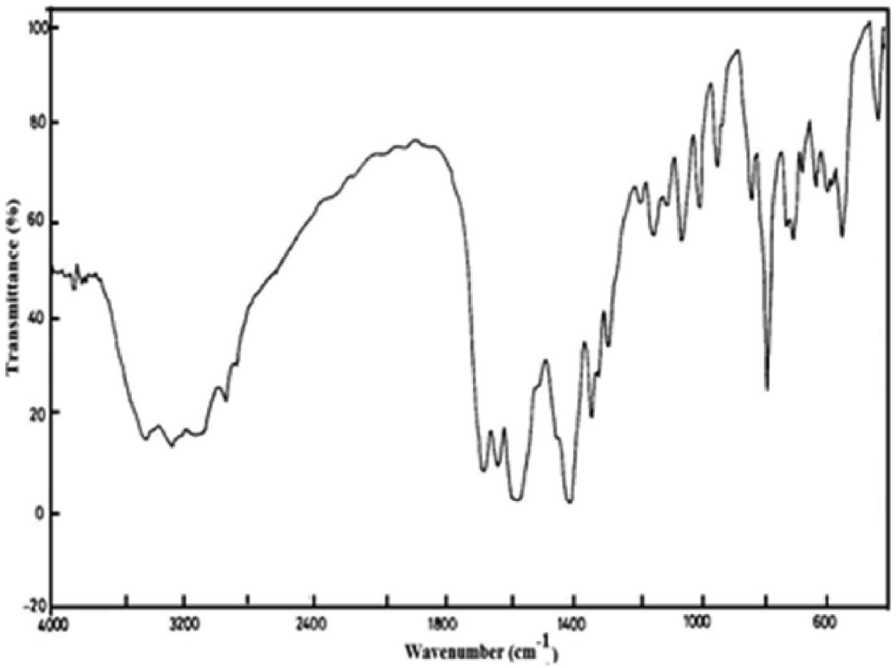

Fig. 2 FTIR spectra of [La{2-$C_6H_4(CH_3CONH)COO\}_3.(N_2H_4)$].

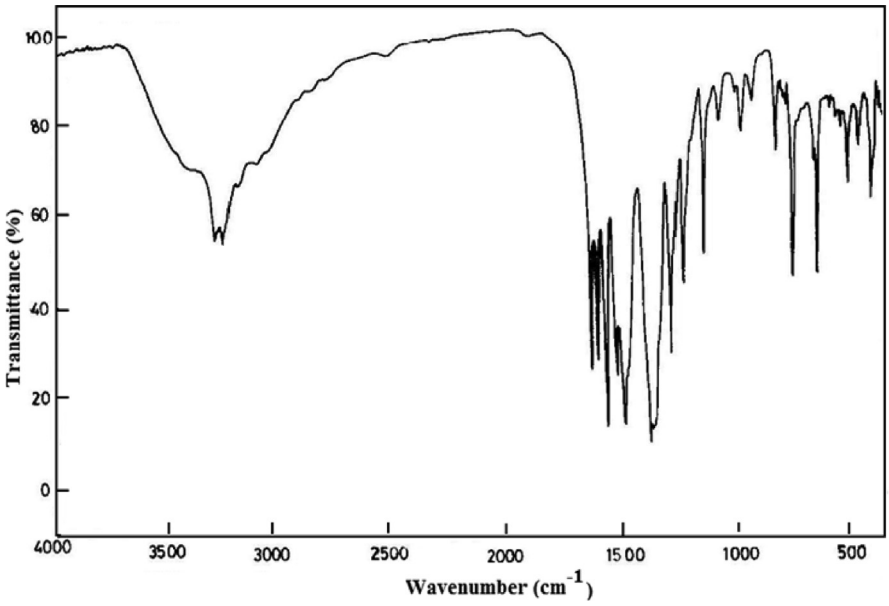

Fig. 3 FTIR spectra of [Nd{3-$C_6H_4(CH_3CONH)COO\}_3.(N_2H_4)$].

3.2.1. FTIR spectra of [Ln {x-$C_6H_4(CH_3CONH)COO\}_3.(N_2H_4)$] where x = 2 or 3 or 4)

The IR spectra of the complexes show $\nu_{C=O\ asym}$ (acid) between 1523 and 1612 cm^{-1} and $\nu_{C=O\ sym}$(acid) between 1393 and 1489 cm^{-1}. The difference of the two frequencies, 122–166 cm^{-1} supports the bidental coordination of carboxylate ions to metal (Nakamoto et al., 2009). The broad absorption peak in the range of 3336 – 3867 cm^{-1} corresponding to ν_{OH} of the acids was not observed in the spectra of the compounds because the carboxylate group was involved in the complex formation. The absorptions at 955–980 cm^{-1} observed in IR of complexes were assigned to $\nu_{N\text{-}N}$ of N_2H_4 present in complexes, which reveals the presence of hydrazine in the form of bridging bidentate coordination mode (Braibanti et al., 1968). The C═O of amide group of the complexes show their stretching at 1632–1709 cm^{-1} which is almost similar to the bands observed for acids, implying that these complexes have no indication of coordination of the amide group with metal. The N-H stretching of hydrazine and N-H of the amide groups are observed to be merging in the regions of 3146–3275 cm^{-1}. Similarly, C═O stretching of the amide is

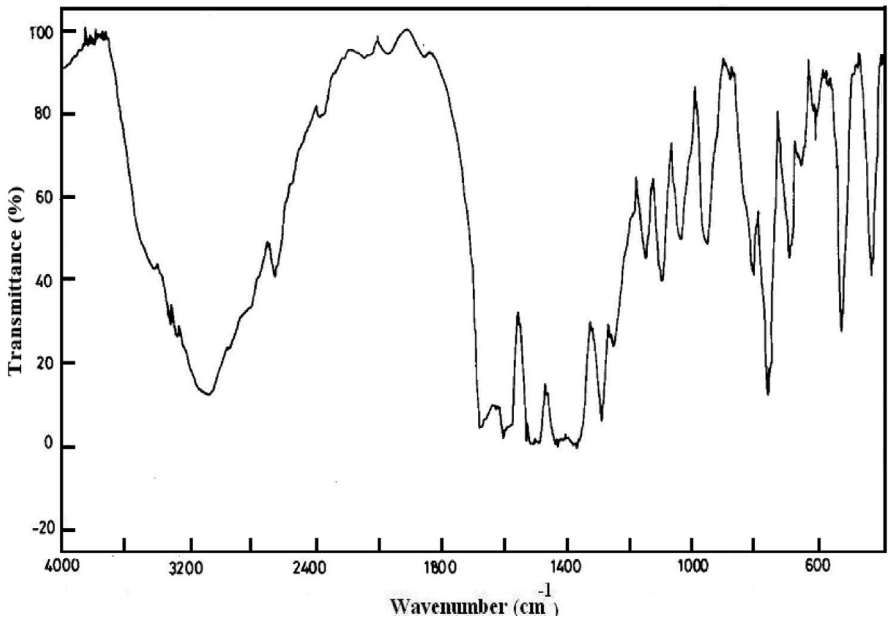

Fig. 4 FTIR spectra of [Gd{4-$C_6H_4(CH_3CONH)COO\}_3.(N_2H_4)$].

Table 4A Thermal data of lanthanide complexes of 2-acetamido benzoic acids and hydrazine.

Complexes	DTA Temp (°C)	Thermogravimetry (TG)			Nature of the reaction
		Temp. Range (°C)	Mass Loss/%		
			Anal.	Calcd.	
Lanthanide complexes of 2-acambH where Ln = La, Ce, Pr, Nd, Sm, and Gd					
[La{2-$C_6H_4(CH_3CONH)COO\}_3(N_2H_4)$]	160.00(-)	60-225	4.30	4.54	Dehydrazination
	255.10(-)				
	412.10(-)	225-450	45.51	45.54	Formation of metal phthalate
	524.10(-)	450-700	76.60	76.91	Decomposition to metal oxide
[Ce{2-$C_6H_4(CH_3CONH)COO\}_3(N_2H_4)$]	134.30(-)	40-180	4.50	4.53	Dehydrazination
	447.50(-)	180-700	76.73	76.80	Decomposition to metal oxide
[Pr{2-$C_6H_4(CH_3CONH)COO\}_3(N_2H_4)$]	85.60(-)	40-200	4.70	4.52	Dehydrazination
	268.30(-)				
	418.60(-)	200-440	45.00	45.30	Formation of metal phthalate
	532.10(-)	440-700	76.00	75.97	Decomposition to metal oxide
[Nd{2-$C_6H_4(CH_3CONH)COO\}_3(N_2H_4)$]	100.00(-)	60-140	4.70	4.50	Dehydrazination
	240.00(-)				
	417.40(-)	140-470	45.00	45.01	Formation of metal phthalate
	522.10(-)	470-700	76.00	76.40	Decomposition to metal oxide
[Sm{2-$C_6H_4(CH_3CONH)COO\}_3(N_2H_4)$]	180.00(-)	60-200	4.37	4.46	Dehydrazination
	240.00(-)	200-430	44.59	44.71	Formation of metal phthalate
	490.60(-)	430-700	75.83	75.68	Decomposition to metal oxide
[Gd{2-$C_6H_4(CH_3CONH)COO\}_3(N_2H_4)$]	100.00(-)	60-240	4.60	4.40	Dehydrazination
	310.00(-)	240-460	44.10	44.30	Formation of metal phthalate
	557.30(-)	460-700	75.00	75.02	Decomposition to metal oxide

Table 4B Thermal data of lanthanide complexes of 3-acetamido benzoic acids and hydrazine.

Complexes	DTA Temp (°C)	Thermogravimetry (TG)			Nature of the reaction
		Temp. Range(°C)	Mass Loss/%		
			Anal.	Calcd.	
Lanthanide complexes of 3-acambH where Ln = La, Ce, pr, Nd, Sm and Gd					
$[La\{3\text{-}C_6H_4(CH_3CONH)COO\}_3(N_2H_4)]$	85.30(-) 240.00(-) 424.70(-) 482.60(-)	40-200 200-440 440-700	4.95 45.34 77.00	4.54 45.44 76.91	Dehydrazination Formation of metal phthalate Decomposition to metal oxide
$[Ce\{3\text{-}C_6H_4(CH_3CONH)COO\}_3(N_2H_4)]$	85.70(-) 200.00(-) 540.00(-)	60-180 180-700	4.62 75.70	4.53 75.80	Dehydrazination Decomposition to metal oxide
$[Pr\{3\text{-}C_6H_4(CH_3CONH)COO\}_3(N_2H_4)]$	100.00 (-) 328.60 (-) 417.60 (-) 560.00(-)	40-160 160-460 460-700	4.62 38.46 76.20	4.52 38.59 75.97	Dehydrazination Formation of metal phthalate Decomposition to metal oxide
$[Nd\{3\text{-}C_6H_4(CH_3CONH)COO\}_3(N_2H_4)]$	97.00(-) 169.80(+) 274.00(-) 417.60(-) 507.30(-)	60-160 160-460 460-700	4.60 76.00	4.50 76.33	Dehydrazination Formation of unstable intermediate Decomposition to metal oxide
$[Sm\{3\text{-}C_6H_4(CH_3CONH)COO\}_3(N_2H_4)]$	140.00(-) 229.00(-) 425.60(-) 506.10(-)	30-200 200-460 460-700	4.29 44.61 76.19	4.46 44.72 76.33	Dehydrazination Formation of metal phthalate Decomposition to metal oxide
$[Gd\{3\text{-}C_6H_4(CH_3CONH)\ COO\}_3(N_2H_4)]$	120.00(-) 171.80(-) 432.90(-) 572.00(-)	60-160 160-460 460-700	4.38 44.00 74.75	4.42 44.32 74.94	Dehydrazination Formation of metal phthalate Decomposition to metal oxide

also found to be overlapping that of C═O of carboxylate ion, which was observed in the region 1632–1709 cm^{-1} respectively, which could not be differentiated.

3.3. Thermal studies

Simultaneous TG-DTA data of the complexes are summarized in Table 4. The compositions of the intermediates and the final products are those which best fit with the observed mass losses in the TG studies, and are in good agreement with the corresponding DTA data. The thermograms are shown in Figs. 5–7.

All the complexes undergo almost similar type of degradation pattern. The complexes show three step decompositions as recorded by TG, namely, dehydrazination, decomposition of lanthanide carboxylate to phthalate intermediate and decomposition of phthalate intermediate to metal oxides. Though the thermograms of Cerium complexes show similar pattern of decomposition, the intermediate was unstable and unidenti-

Table 4C Thermal data of lanthanide complexes of 4-acetamido benzoic acids and hydrazine.

Complexes	DTA Temp(°C)	Thermogravimetry (TG)			Nature of the reaction
		Temp. Range(°C)	Mass Loss/%		
			Anal.	Calcd.	
Lanthanide complexes of 4-acambH where Ln = La, Ce, pr, Nd, Sm and Gd					
[La{4-$C_6H_4(CH_3CONH)COO\}_3(N_2H_4)$]	52.00(+)	40-110	4.41	4.54	Dehydrazination
	130.00(-) }				
	420.00(-)	110-440	47.70	47.79	Formation of metal phthalate
	549.00(-)	440-700	77.00	77.91	Decomposition to metal oxide
[Ce{4-$C_6H_4(CH_3CONH)COO\}_3(N_2H_4)$]	85.00(-)	50-200	4.62	4.53	Dehydrazination
	248.00(-)				
	300.00(-)	200-700	76.72	76.80	Decomposition to metal oxide
	428.00(-)				
[Pr{4-$C_6H_4(CH_3CONH)COO\}_3(N_2H_4)$]	83.00(+)	83-200	4.30	4.52	Dehydrazination
	216.00(-)	200-244	10.00	10.88	Removal of NH group
	370.00(-) }				
	496.00(-)	244-507	45.10	45.30	Formation of metal phthalate
	557.00(-)	507-700	76.00	75.95	Decomposition to metal oxide
[Nd{4-$C_6H_4(CH_3CONH)COO\}_3(N_2H_4)$]	81.00(+)	50-185	5.00	4.50	Dehydrazination
	214.00(-)	185-250	10.77	10.83	Removal of NH group
	429.00(-)	250-485	42.30	45.14	Formation of metal phthalate
	536.00 (-)	485-700	77.70	77.80	Decomposition to metal oxide
[Sm{4-$C_6H_4(CH_3CONH)COO\}_3(N_2H_4)$]	93.00(+)	60-180	44.61	4.46	Dehydrazination
	211.00(-)	180-346	10.70	10.74	Removal of NH group
	367.00(-) }				
	452 .00(-)	346-481	45.40	44.72	Formation of metal phthalate
	559.00(-)	481-700	76.00	75.68	Decomposition to metal oxide
[Gd{4-$C_6H_4(CH_3CONH)COO\}_3(N_2H_4)$]	111.00(+)	60-200	4.60	4.40	Dehydrazination
	211.00(-)	200-396	10.80	10.60	Removal of NH group
	442.00(-)	396-500	44.10	44.30	Formation of metal phthalate
	542.00(-)	500-700	74.95	75.00	Decomposition to metal oxide

(+) – endo, (-) – exo, (Anal.) – Analytical& (Calcd.) – Calculated

(+) – endo, (–) – exo, (Anal.) – Analytical& (Calcd.) – Calculated.

fiable. Dehydrazination occur showing endotherms in the range of 52 to 111 °C in case of 4-acambH complexes. Exothermic dehydrazination is observed for 2-acambH and 3-acambH complexes in the range 85 to 180 °C. This may be due to stability of the formation of the former than the latter two. In case of lanthanum complexes of 4-acambH the dehydrazinated metal carboxylates undergo exothermic decomposition showing exothermic peaks in the range of 172 to 370 °C and 412 to 496 °C to metal phthalates. The mass loss percentage indicates phthalates formation. The decomposition temperature of these intermediates more or less going along with the values reported (Gorgola and Brzyska, 1999). The Neodymium complex of 3-acetamido benzoate decomposes directly into its metal oxide, whose intermediate is found to be unstable, which could not be identified. Metal phthalates finally undergo oxidative decomposition showing broad exotherms in the range of 428 to 572 °C to the metal oxide residues.

All cerium complexes show dehydrazination in the first step. As in the other cases, 4-acambH complexes show endothermic dehydrazination. After dehydrazination, cerium complexes decompose to their corresponding metal oxide with no stable intermediate formation.

Among the praseodymium complexes, thermogram of 4-isomer has registered an additional exotherm at 216 °C indicating the removal of NH group prior to the formation of the phthalate intermediate. This trend is also observed in other complexes like Nd, Sm and Gd of the same isomeric benzoate. The decomposition steps involved were given in equations 2–5. The decomposition path was followed by analyzing the decompositions of 4-acetamido samarium complex at different steps using IR spectra. The IR spectra of the intermediates of 4 -acmbH of samarium complex are shown in Figs. 8–11. The IR spectra of the intermediate (1) after heating the sample to 93 °C, intermediate (2) after heating the sample to 211 °C,

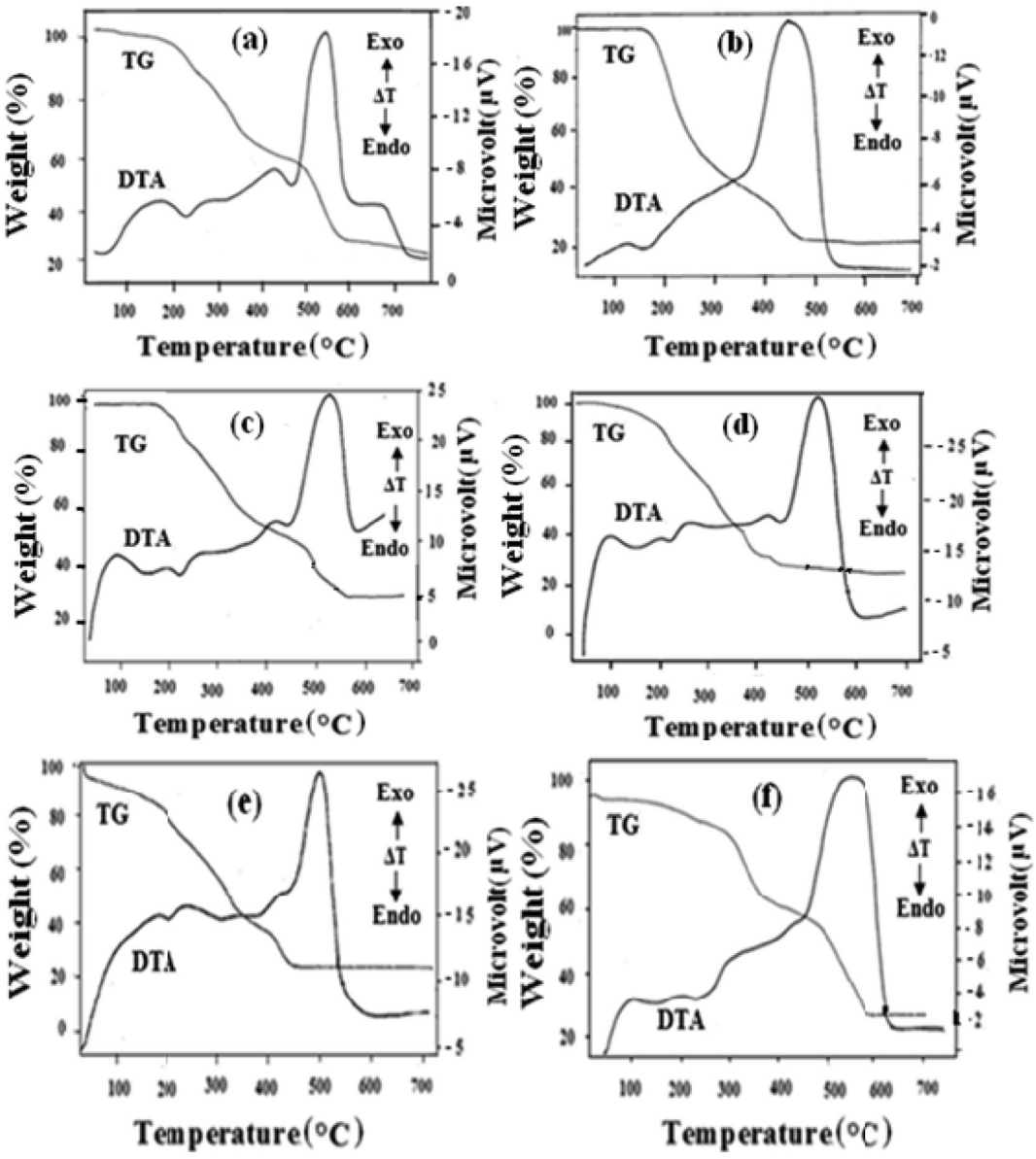

Fig. 5 TG-DTA curves of Metal Hydrazine complexes: (a) [La{2-$C_6H_4(CH_3CONH)COO\}_3.(N_2H_4)$]; (b) [Ce{2-$C_6H_4(CH_3CONH)COO\}_3.(N_2H_4)$]; (c) [Pr{2-$C_6H_4(CH_3CONH)COO\}_3.(N_2H_4)$]; (d)[Nd{2-$C_6H_4(CH_3CONH)COO\}_3.(N_2H_4)$]; (e) [Sm{2-$C_6H_4(CH_3CONH)COO\}_3.(N_2H_4)$]; (f)[Gd{2-$C_6H_4(CH_3CONH)COO\}_3.(N_2H_4)$.

intermediate (3) after heating the sample to 367 °C and the intermediate (4) after heating the sample to 452 °C were analyzed for their characteristic peaks. The spectra of the intermediates reveal that N-N stretching of the NH moiety and the NH frequency of the amide group disappear gradually by forming broad peaks. The IR results of intermediate (4) shows $\nu_{C=O(asym)}$ band at 1582 cm^{-1} and $\nu_{C=O(sym)}$ band at 1495 cm^{-1}, which are the characteristic frequencies of phthalate ion (Nakamoto et al., 2009; Braibanti et al., 1968). The decomposition steps involved are given below.

Reaction scheme 1:

$$[Ln\{x\text{ - }C_6H_4(NHCOCH_3)COO\}\ N_2H_4] \overset{50-180^{\circ}C}{\rightarrow} [Ln(x\text{ - }C_6H_4(NHCOCH_3)COO)_3] + N_2 + 2H_2 \quad (2)$$

where Ln = La, Ce, Pr, Nd, Sm & Gd

= 2 (or) 3 (or) 4 - acetamidobenzoic acid

$$[Ln\{\ x\text{ - }C_6H_4(NHCOCH_3)COO\}_3]\ +\ 10\ 1/2\ O_2 \xrightarrow{172-496^{\circ}C} [Ln\{\ (x\text{ - }C_6H_4(COO)_2\}_3]\ +\ 3CO_2 + 12H_2O +\ 1/2\ N_2 \quad (3)$$

where Ln = La, Pr, Nd, Sm & Gd.

$$2[Ln\{\ (x\text{ - }C_6H_4(COO)_2\}_3]\ +\ 43\ 1/2\ O_2 \xrightarrow{483-572^{\circ}C} Ln_2O_3 + 48CO_2 + 12H_2O \quad (4)$$

where Ln = La, Pr, Nd, Sm & Gd.

Reaction scheme 2:

$$2[Ce\{\ (2)/(3)/(4)\text{ - }C_6H_4(NHCOCH_3)COO\}_3]\ +\ 59O_2 \xrightarrow{428-540^{\circ}C} 2CeO_2 + 54CO_2 + 24H_2O\ +\ N_2 \quad (5)$$

The remaining IR spectras of 15 isomeric complexes are presented in the supplement index.

3.4. X-Ray diffraction studies

The powder XRD patterns along with their d-spacings are given in Table 5. The comparison of XRD patterns of the lanthanides are shown in Figs. 12–14. The XRD patterns of acetamidobenzoate lanthanides series reveal that each set of acetamidobenzoic acid complexes has similarities in their structures implying similar compositions. The powder XRD patterns of the 2 and 3-isomeric complexes exhibit more or less sharp peaks indicating polycrystalline nature whereas the X-

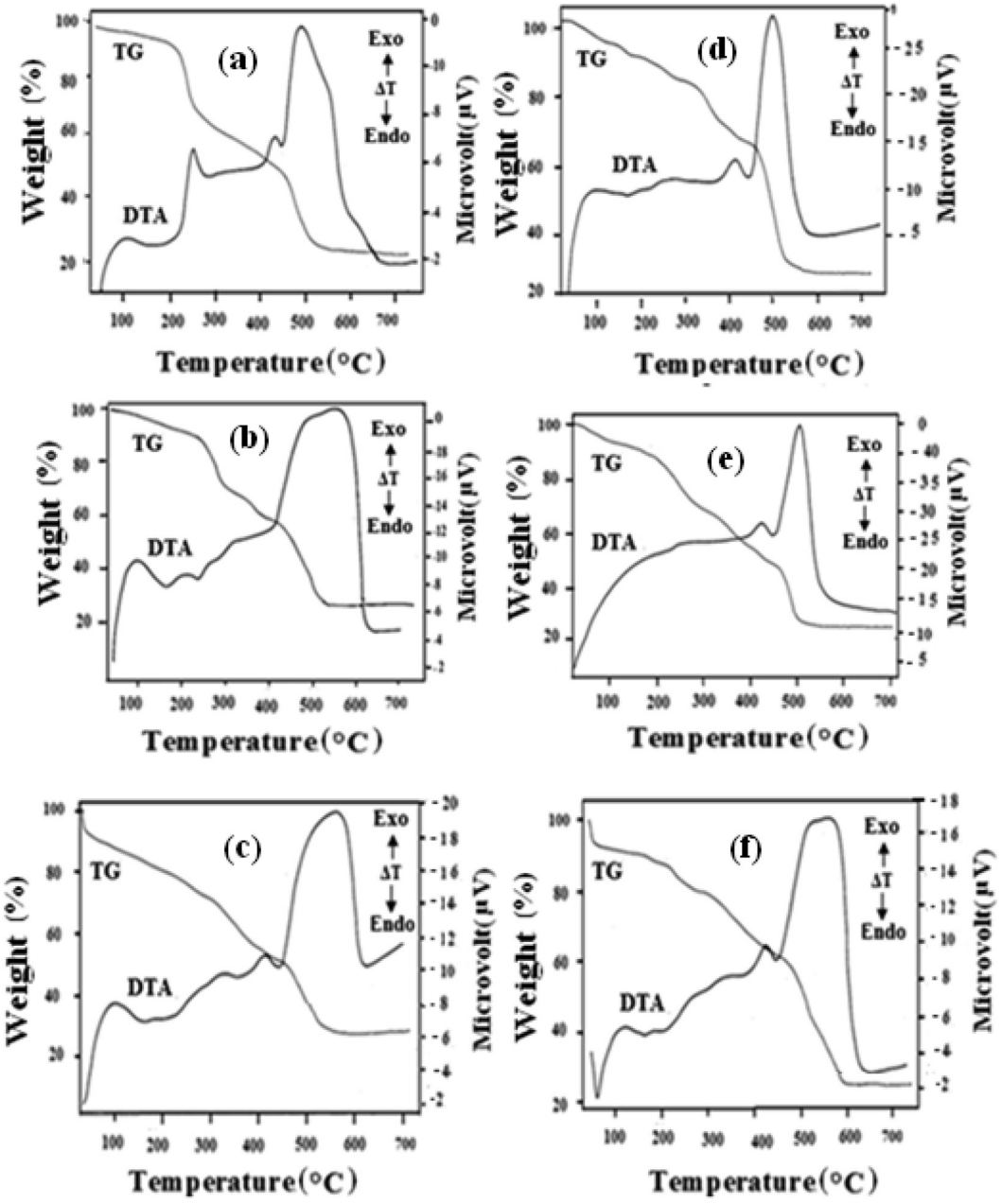

Fig. 6 TG-DTA curves of Metal Hydrazine complexes.(a) [La{3-$C_6H_4(CH_3CONH)COO\}_3.(N_2H_4)$]; (b) [Ce{3-$C_6H_4(CH_3CONH)COO\}_3.(N_2H_4)$]; (c) [Pr{3-$C_6H_4(CH_3CONH)COO\}_3.(N_2H_4)$]; (d) [Nd{3-$C_6H_4(CH_3CONH)COO\}_3.(N_2H_4)$]; (e) [Sm{3-$C_6H_4(CH_3CONH)COO\}_3.(N_2H_4)$]; (f) [Gd{3-$C_6H_4(CH_3CONH)COO\}_3.(N_2H_4)$].

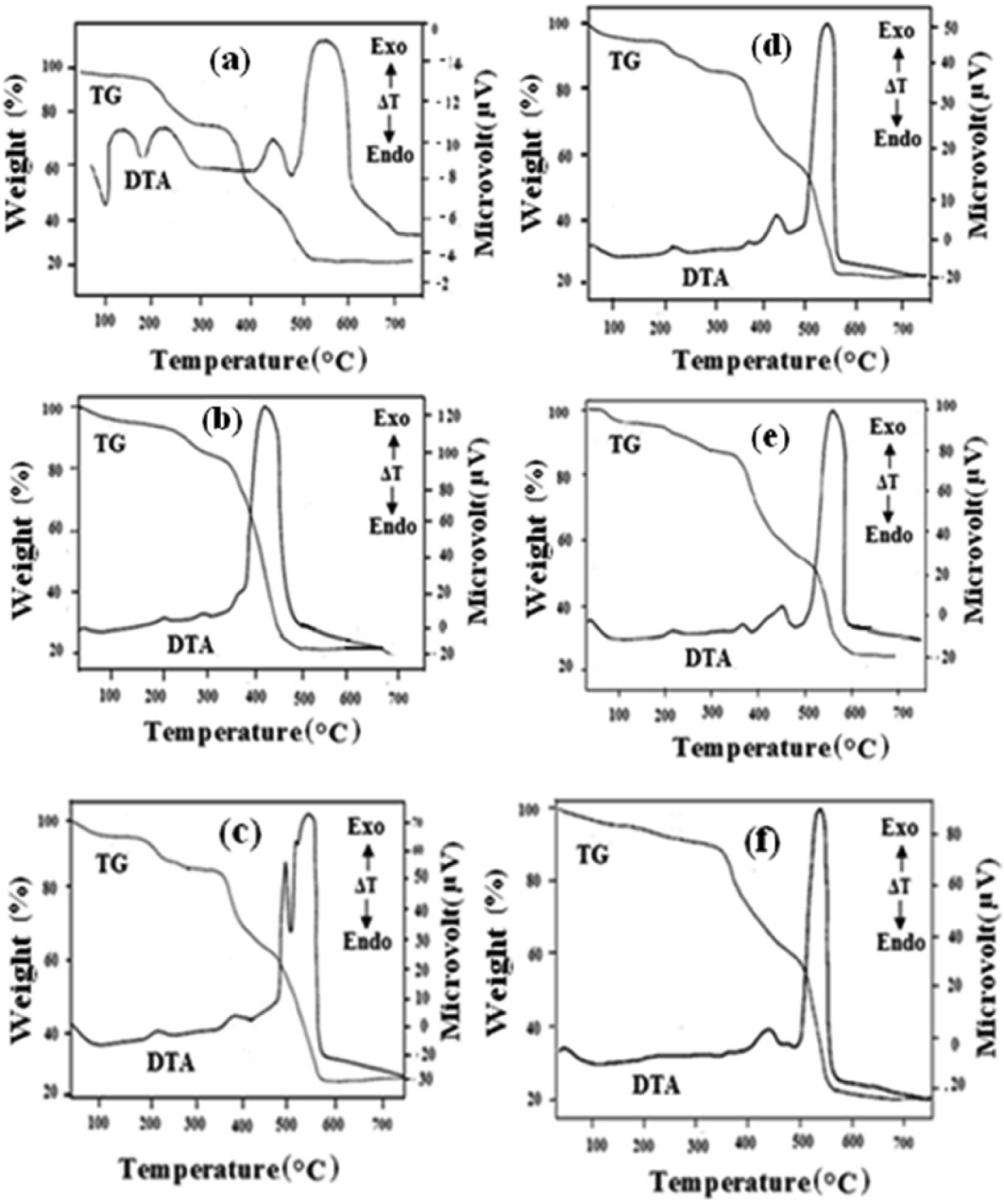

Fig. 7 TG-DTA curves of Metal Hydrazine complexes: (a)[La{4-$C_6H_4(CH_3CONH)COO\}_3.(N_2H_4)$]; (b) [Ce{4-$C_6H_4(CH_3CONH)COO\}_3.(N_2H_4)$]; (c) [Pr{4-$C_6H_4(CH_3CONH)COO\}_3.(N_2H_4)$]; (d) [Nd{4-$C_6H_4(CH_3CONH)COO\}_3.(N_2H_4)$]; (e) [Sm{4-$C_6H_4(CH_3CONH)COO\}_3.(N_2H_4)$]; (f) [Gd{4-$C_6H_4(CH_3CONH)COO\}_3.(N_2H_4)$].

ray pattern of the 4-isomeric lanthanide complexes display wide and weak intensity peaks may be due to smaller particle sizes. All substances are found to be crystalline and complexes of 2, 3 isomeric acids show more crystallinity. Correlation studies of the X-ray patterns were subsequently used to confirm that the above products were single-phase materials. However, they display similar patterns implying isomorphism. Their particle sizes were substantiated by SEM- EDAX analysis (Gaye, et al., 2003). With the justification of analytical, magnetic, spectral, thermal and XRD characterizations the eight coordination sites were ascribed around the Ln^{3+} ions. Among the eight coordinated sites six were occupied by three bidentate acetamido benzoate moieties and the rest of two sites were inhabited by two bridging bidentate hydrazine groups.

3.5. SEM–EDAX studies

It is generally observed that the hydrazine complexes yield metal oxides of nano scale on decomposition, due to their explosive nature (ref). Similar study was undertaken by decomposing the complexes in muffle furnace at their decomposition temperatures (observed from thermal analysis), keeping them

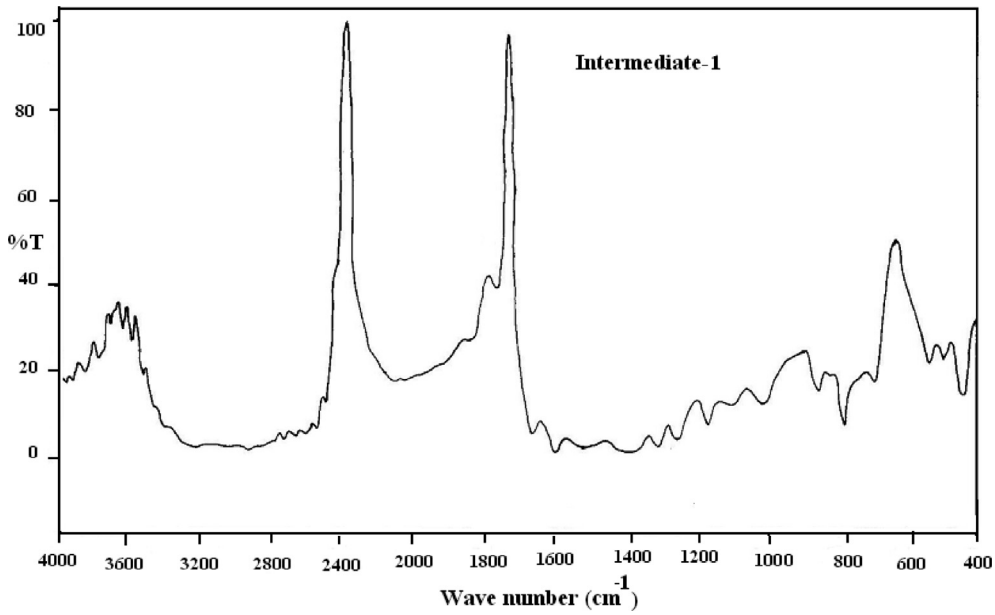

Fig. 8 FTIR analysis of intermediate −1 of [Sm{4-C_6H_4(CH_3CONH)COO}$_3$.(N_2H_4)].

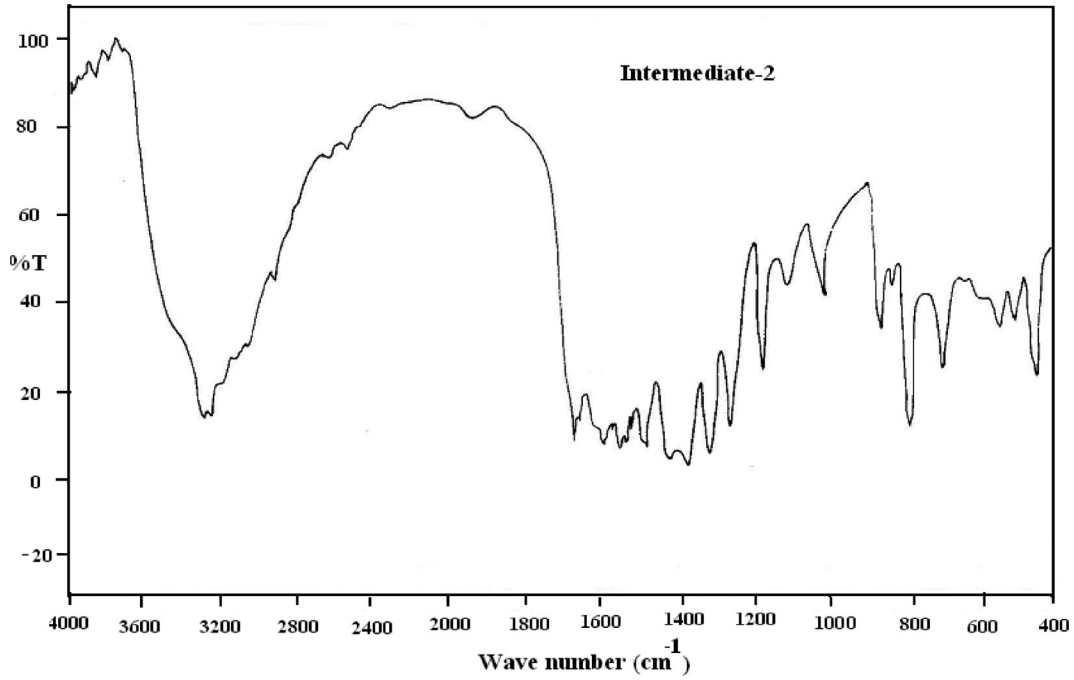

Fig. 9 FTIR analysis of intermediate-2 of [Sm{4-C_6H_4(CH_3CONH)COO}$_3$.(N_2H_4)].

at the same temperature for 30 min., and analyzing for their morphology and particle size of the residual oxides using SEM EDAX studies. Owing to the breaking of hydrazine and exothermic decomposition of organic moiety, the residues were of irregular shapes as evidenced by their SEM images. The SEM–EDAX pictures of Nd_2O_3 and Pr_6O_{11} confirmed the existence of corresponding metals presented in Figs. 15–20. A comparison between the SEM–EDAX pictures of residues with the reported nano-neodymium and praseodymium oxides (Figs. 16, 18), shows that they display similar spectra, supporting the existence of the corresponding rare earth metal in the compounds as reported (Lembang et al., 2018; Pourmortazavi et al., 2017). The size of metal oxide particles lie in the range of 1–10 μm due to the insufficient quantity of hydrazine in the complex to decompose to oxides of nano scale.

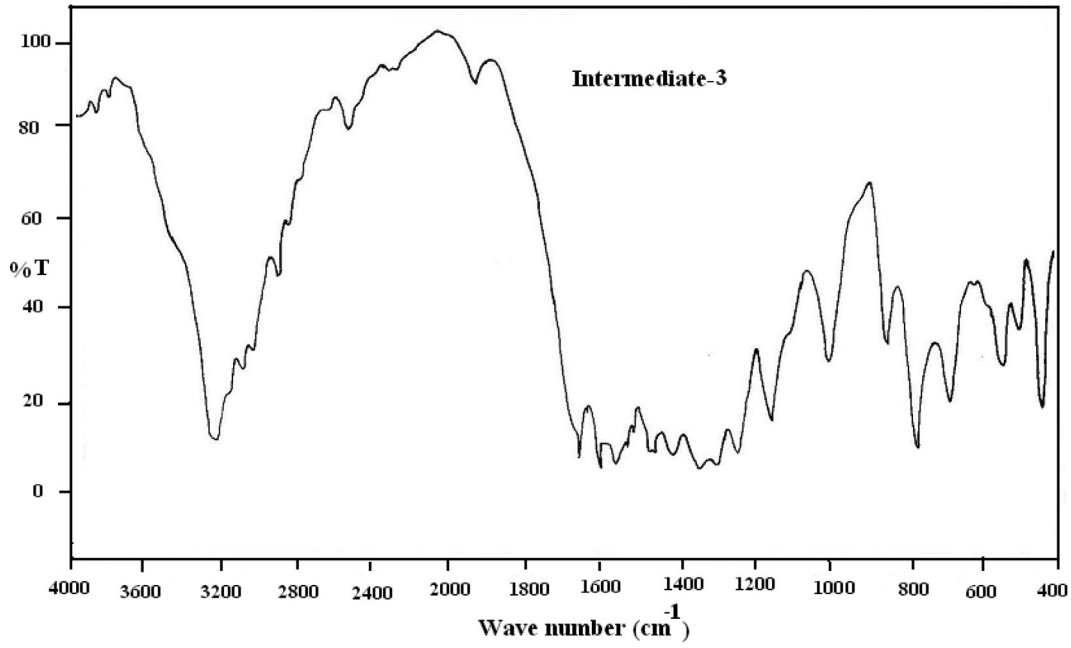

Fig. 10 FTIR analysis of intermediate- 3 of [Sm{4-$C_6H_4(CH_3CONH)COO\}_3.(N_2H_4)$].

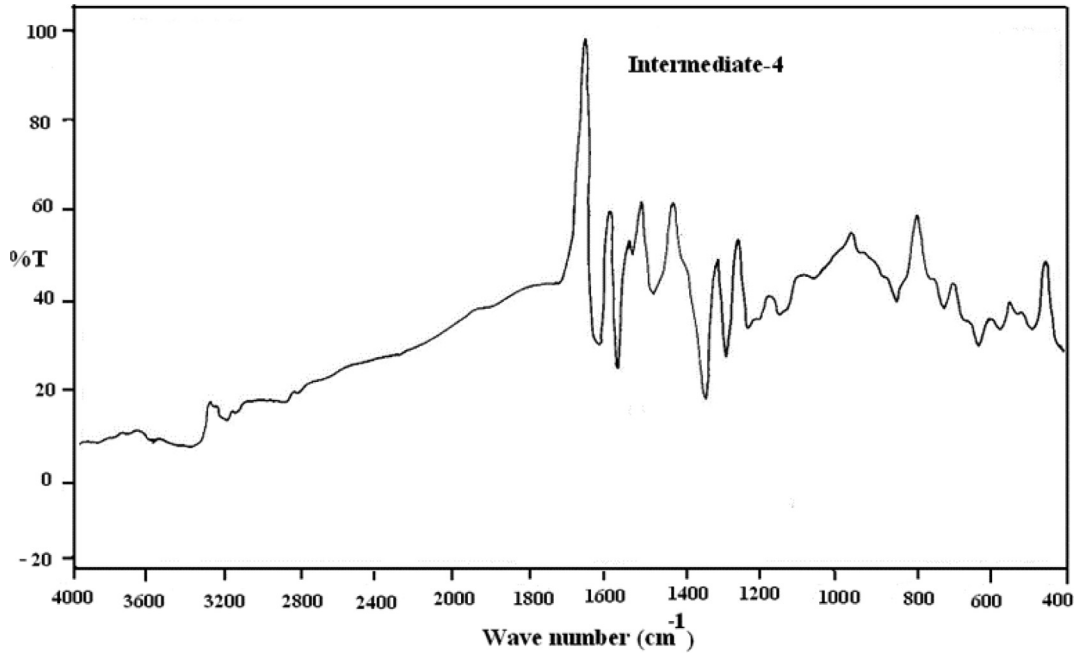

Fig. 11 FTIR analysis of intermediate- 4 of [Sm{4-$C_6H_4(CH_3CONH)COO\}_3.(N_2H_4)$].

3.6. Conductance studies

Conductance of hydrazine complexes lanthanide metal complexes of isomeric acetamido benzoic acids was measured by solution method using DMSO as solvent. Solutions of complexes were prepared in DMSO and specific conductance was measured first and then molar conductance was calculated as in the case of transition metal complexes the values are given in Table 6. The molar conductance values are found to be in the range of 8–20 $O^{-1}cm^2mol^{-1}$ indicating that these compounds are neutral complexes (Geary, 1971; Ramalingam and Soundararajan, 1967).

3.7. ^{13}C and ^{1}H - NMR spectral studies

To ascertain the presence acid moiety in the complexes, ^{13}C – NMR spectra were recorded and given in Fig. 22. In

Table 5A X-ray diffraction data of lanthanide complexes of 2-aceatamido benzoate and hydrazine (D spacing in Å units and intensity in parentheses).

$[Ln\{2\text{-}C_6H_4(CH_3CONH)COO\}_3(N_2H_4)]$where Ln = La, Ce, Pr, Nd, Sm and Gd for 2-acambH					
La	Ce	Pr	Nd	Sm	Gd
12.78(100.00)	12.90(100.00)	12.86(49.30)	17.90(100.00)	13.05(100.00)	11.54(91.30)
8.05(10.30)	7.54(19.20)	7.40(32.80)	8.07 (8.30)	8.11(6.70)	10.07(78.30)
7.51 (14.70)	6.56(9.60)	6.44(23.90)	7.53(21.70)	7.59(15.00)	7.83(26.10)
6.54(7.40)	5.70(11.50)	5.61(29.90)	6.54(11.70)	6.59(6.70)	7.29(32.60)
5.69(8.80)	5.24(9.60)	4.91(100.00)	5.69(11.70)	5.72(6.70)	6.35(19.60)
5.23((5.80)	4.97(36.50)	4.62(16.40)	5.22(6.70)	4.99(20.00)	5.82(26.10)
4.97(26.50)	4.39(15.38)	4.35(37.30)	4.96(40.00)	4.41(10.00)	5.19((4.60)
4.39(17.60)	3.82(26.90)	3.79(55.20)	4.68(8.30)	4.06(5.00)	4.71(52.20)
4.15(5.80)	3.47(23.10)	3.43(38.80)	4.38(21.70)	3.83(15.00)	4.49(56.50)
3.92(8.80)	2.89(7.70)	3.19(26.90)	3.82(23.30)	3.47(6.70)	4.24(52.20)
3.84(23.50)	2.73(9.60)	3.11(23.90)	3.37(10.00)	3.15(6.70)	4.04(45.70)
3.34(7.40)	2.60(19.60)	2.87(19.40)	3.13(11.70)	2.89(6.70)	3.87(43.50)
3.14(16.20)		2.70(20.90)	2.88(8.30)	2.73(6.70)	3.58(37.00)
2.90(5.80)		2.59(23.90)	2.72(8.30)	2.61(6.70)	3.32(67.40)
2.51(5.80)		2.48(14.90)	2.60(8.30)	2.50(5.00)	3.14(28.30)
1.95(1.50)		2.30(17.90)	2.30(6.70)	2.32(5.00)	2.48(23.90)
		2.24(11.90)		2.07(5.00)	2.21(23.90)
		2.04(17.90)			2.03(15.20)
					2.00(19.60)

Table 5B X-ray diffraction data of lanthanide complexes of 3-aceatamido benzoate and hydrazine (D spacing in Å units and intensity in parentheses).

$[Ln\{3\text{-}C_6H_4(CH_3CONH)COO\}_3(N_2H_4)]$where Ln = La,Ce, Pr, Nd, Sm and Gd for 3-acambH					
La	Ce	Pr	Nd	Sm	Gd
13.71(45.50)	14.03(17.50)	9.99(14.75)	13.60(23.53)	9.73(9.09)	9.26(24.59)
12.29(100.00)	12.63(49.12)	9.42(29.51)	12.19(100.00)	9.15(14.55)	7.21(4.92)
9.22(7.27)	11.57(3.50)	7.33(6.56)	9.81(7.84)	7.15(7.27)	5.57(14.75)
7.71(25.50)	10.02(10.50)	5.67(19.67)	9.22(11.76)	5.58(18.18)	5.28(100.00)
7.01(18.10)	9.43(22.80)	5.35(100.00)	7.68(13.70)	5.25(100.00)	5.11(34.43)
6.19(3.64)	7.85(22.80)	4.73(29.50)	7.18(7.84)	5.08 (29.09)	4.66(32.79)
5.62(10.91)	7.28(7.02)	4.17(21.31)	6.96(15.69)	4.65(25.45)	4.13(19.67)
5.26(38.18)	5.67(17.50)	3.83(14.75)	6.18(3.92)	4.12(23.64)	3.65(29.50)
4.90(54.50)	5.36(100.00)	3.68(83.61)	5.59(17.65)	3.78(9.09)	3.39(21.31)
4.21(25.50)	5.18(38.60)	3.41(54.09)	5.27(56.86)	3.62(52.73)	3.32(24.59)
3.89(14.50)	4.97(29.82)	3.17(37.70)	4.86(31.37)	3.38(45.45)	3.15(22.95)
3.63(60.00)	4.73(35.09)	3.11(42.62)	4.66(27.45)	3.32(32.73)	2.50(1.48)
3.39(38.18)	3.93(5.26)	2.60(9.84)	4.19(27.45)	3.08(40.00)	2.46(6.56)
3.08(32.70)	3.67(31.58)	2.52(13.11)	4.04(19.60)	2.49(23.64)	2.03(8.20)
2.87(7.27)	3.42(26.32)	2.48(8.20)	3.88(9.80)	2.46(9.09)	
2.70(9.09)	3.36(26.30)	2.04(8.20)	3.62(50.98)	2.05(10.91)	
2.55(10.91)	3.17(15.79)		3.49(17.65)		
2.50(10.91)	3.11)21.05)		3.38(45.10)		
2.42(10.91)	2.89(21.00)		3.29(19.60)		
2.35(14.50)	2.52(15.79)		3.09(2.94)		
2.28(12.73)	2.64(8.77)		2.99(7.84)		
2.23(9.09)			2.69(11.76)		
2.12(9.09)			2.60(3.92)		
2.06(10.90)			2.53(9.80)		
			2.46(15.69)		
			2.41(9.80)		

the spectra of the complexes, $[La\{2\text{-}C_6H_4(NHCOCH_3)COO\}_3(N_2H_4)]$, $[Gd\{3\text{-}C_6H_4(NHCOCH_3)COO\}_3(N_2H_4)]$ & $[La\{4\text{-}C_6H_4(NHCOCH_3)COO\}_3(N_2H_4)]$, the important features noticed are, ^{13}C- NMR (600 MHz, DMSO) On analyzing ^{13}C - NMR spectra, the important characteristic peaks exhibited by the complexes are listed in Table 7 which are similar to

Table 5C X-ray diffraction data of lanthanide complexes of 4-aceatamido benzoate and hydrazine (D spacing in Å units and intensity in parentheses).

$[Ln\{4\text{-}C_6H_4(CH_3CONH)COO\}_3(N_2H_4)]$where Ln = La,Ce, Pr, Nd, Sm and Gd for 4-acambH					
La	Ce	Pr	Nd	Sm	Gd
15.45(100.00)	21.75(57.70)	15.48(100.00)	15.35(100.00)	15.48(100.00)	16.64(100.00)
8.38(16.20)	15.50(96.10)	8.35(22.60)	8.23(20.00)	10.30(4.80)	9.93(8.70)
	8.56(26.90)	7.03(16.10)		8.44(23.80)	8.47(56.50)
	4.87(100.00)	5.48(22.60)		7.30(28.60)	6.62(28.30)
	3.66(57.70)	4.89(25.80)	3.65(16.10)	6.65(28.60)	5.65(23.90)
	3.41(53.80)	3.66(16.10)		5.50(33.30)	4.61(26.10)
				4.70(28.60)	3.65(15.20))

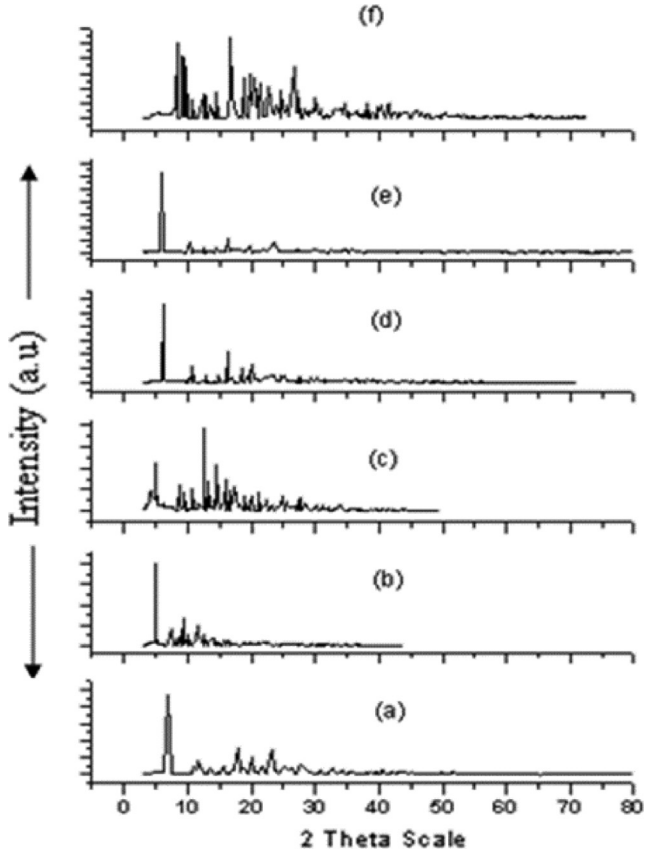

Fig. 12 XRD patterns of Metal Hydrazine complexes: (a) $[La\{2\text{-}C_6H_4(CH_3CONH)COO\}_3.(N_2H_4)]$; (b) $[Ce\{2\text{-}C_6H_4(CH_3CONH)COO\}_3.(N_2H_4)]$; (c) $[Pr\{2\text{-}C_6H_4(CH_3CONH)COO\}_3.(N_2H_4)]$; (d) $[Nd\{2\text{-}C_6H_4(CH_3CONH)COO\}_3.(N_2H_4)]$; (e) $[Sm\{2\text{-}C_6H_4(CH_3CONH)COO\}_3.(N_2H_4)]$; (f) $[Gd\{2\text{-}C_6H_4(CH_3CONH)COO\}_3.(N_2H_4)]$.

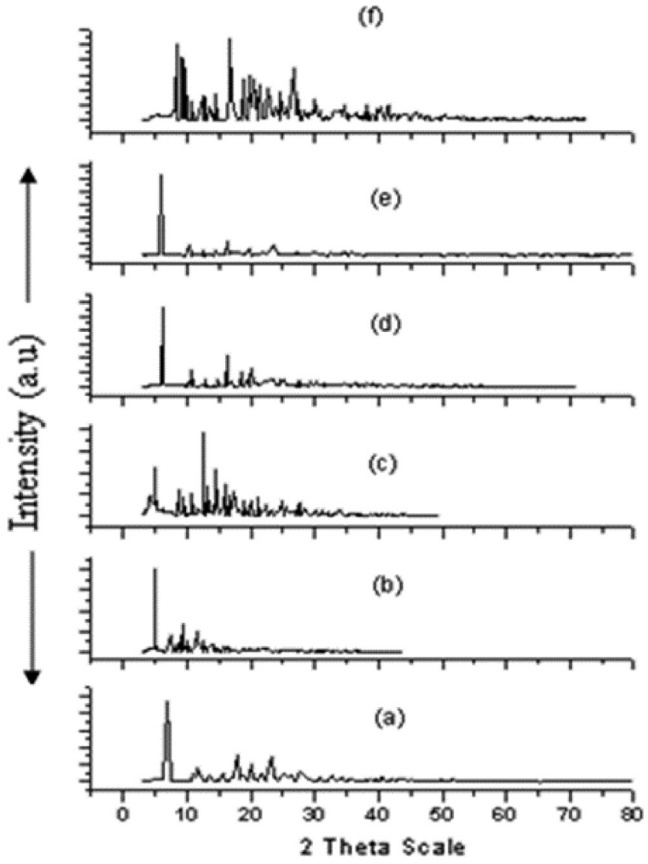

Fig. 13 XRD patterns of Metal Hydrazine complexes. (a) $[La\{3\text{-}C_6H_4(CH_3CONH)COO\}_3.(N_2H_4)]$; (b) $[Ce\{3\text{-}C_6H_4(CH_3CONH)COO\}_3.(N_2H_4)]$; (c) $[Pr\{3\text{-}C_6H_4(CH_3CONH)COO\}_3.(N_2H_4)]$; (d) $[Nd\{3\text{-}C_6H_4(CH_3CONH)COO\}_3.(N_2H_4)]$; (e) $[Sm\{3\text{-}C_6H_4(CH_3CONH)COO\}_3.(N_2H_4)]$; (f) $[Gd\{3\text{-}C_6H_4(CH_3CONH)COO\}_3.(N_2H_4)$.

that shown by the 4-acetamido benzoic acid Fig. 21 (SDBS No.6318 CDS-01-576,). The observations indicate that the complexes contain acid moiety, which has not undergone any degradation during the preparation of complexes (Abraham and Loftus, 1980).

On evaluating the ^1H - NMR(SDBS No.6318 HSP- 47–33) spectrum of 4-acetamido benzoic acid, majority of the peaks observed are found to be compatible with those of the complexes, which are given in Table 7. ^1H -NMR (600 MHz, DMSO. Since the value of δ 12.8 is ascribed to C1H in the 4-acetamido benzoic acid is vanishes in the complexes implying that the acid moiety is involved in complexation (Milenkovic et al., 2012).

3.8. Mass spectral studies

The mass Spectrum of 4 - acetamido complex was recorded to find out the molecular mass of the complex, as a representative

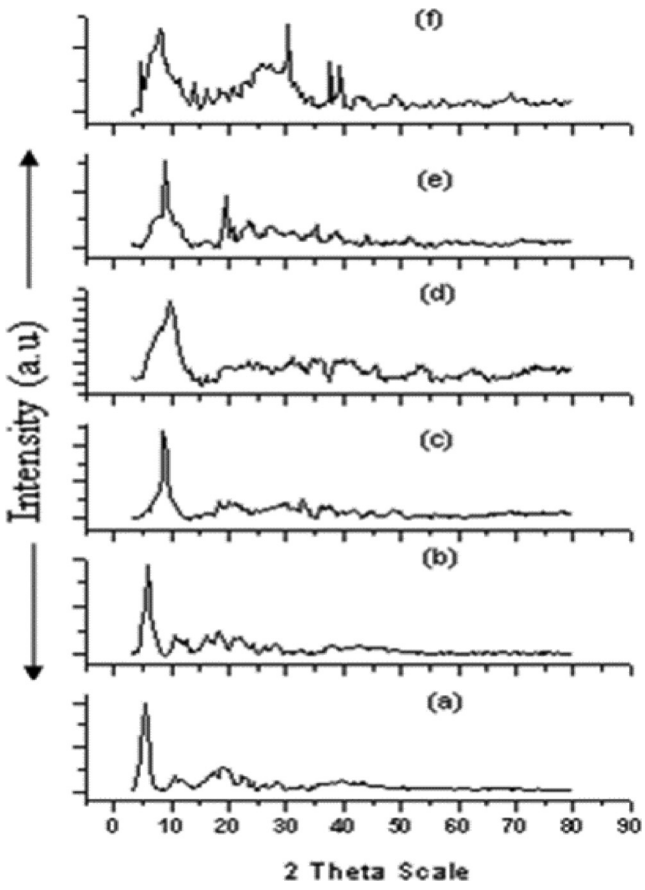

Fig. 14 XRD patterns of Metal Hydrazine complexes: (a) [La{4-$C_6H_4(CH_3CONH)COO\}_3.(N_2H_4)$]; (b) [Ce{4-$C_6H_4(CH_3CONH)COO\}_3.(N_2H_4)$]; (c) [Pr{4-$C_6H_4(CH_3CONH)COO\}_3.(N_2H_4)$]; (d) [Nd{4-$C_6H_4(CH_3CONH)COO\}_3.(N_2H_4)$]; (e) [Sm{4-$C_6H_4(CH_3CONH)COO\}_3.(N_2H_4)$]; (f) [Gd{4-$C_6H_4(CH_3CONH)COO\}_3.(N_2H_4)$].

example. Since the attempt made to obtain the single crystals of the synthesized compounds was not fruitful, the mass spectroscopic characterization was carried out to find the molecular mass of the complexes (Pavia et al., 2015).

The mass Spectrum of 4 - acetamido benzoic acid (NIST number 375119) is correlated with that of the corresponding complex [La{x-$C_6H_4(NHCOCH_3)COO\}_3(N_2H_4)$] shown in Fig. 23. The prominent peaks identified in 4- acetamido benzoic acid with m/z values are 43, 120 and 135 representing the fragments of acyl radical, benzoate radical and phenyl acetamido moieties respectively. The various characteristic fragments of the above-mentioned complex, such as anions, cations and neutral species are listed in Table 7. The prominent peak identified in the spectrum at m/z value of 673, which represents the formula $La\{C_6H_4(CH_3CONH)COO\}_3$ is corresponding to M^+ ion. The m/z value of 59 represents the acetamide (CH_3CONH_2) moiety. The benzoate radical (C_6H_5-COO) is shown by the peak at 121(m/z). Lanthanum metal cation is observed at m/z of 136. The phthalate radical {C_6H_4(-$COO)_2$} ascribed for the m/z value of 166 in the spectrum. A fragment of {$La(C_6H_4(COO)_2$}is observed at m/z 303. Besides, the base peak (most abundant) is corresponding to [(C_7H_4-$O_2)_3.N_2H_4$] moiety is exhibited at m/z 392. As per the spectrum, the molecular ion peak at m/z 1380 accounts for the molecular formula [$La_2\{C_6H_4(NHCOCH_3)COO\}_6$] which was the dimer of the target compound, due its instability the abundance is found to be minimum.

4. Conclusion

The isomeric acetamido benzoic acids undergo reaction with hydrazine hydrate and trivalent lanthanides La^{3+}, Ce^{3+}, Pr^{3+}, Nd^{3+}, Sm^{3+} and Gd^{3+} form complexes of formulae, [Ln{x-$C_6H_4(CH_3CONH)\}_3(N_2H_4)$] at pH 3 and 4.5 (1: 1) ethanolic medium and x = 2, 3, & 4 isomers. The sparingly soluble nature of the formed complexes suggests a polymeric nature through hydrazine bridging substantiated by N-N stretching observed for complexes. All the com-

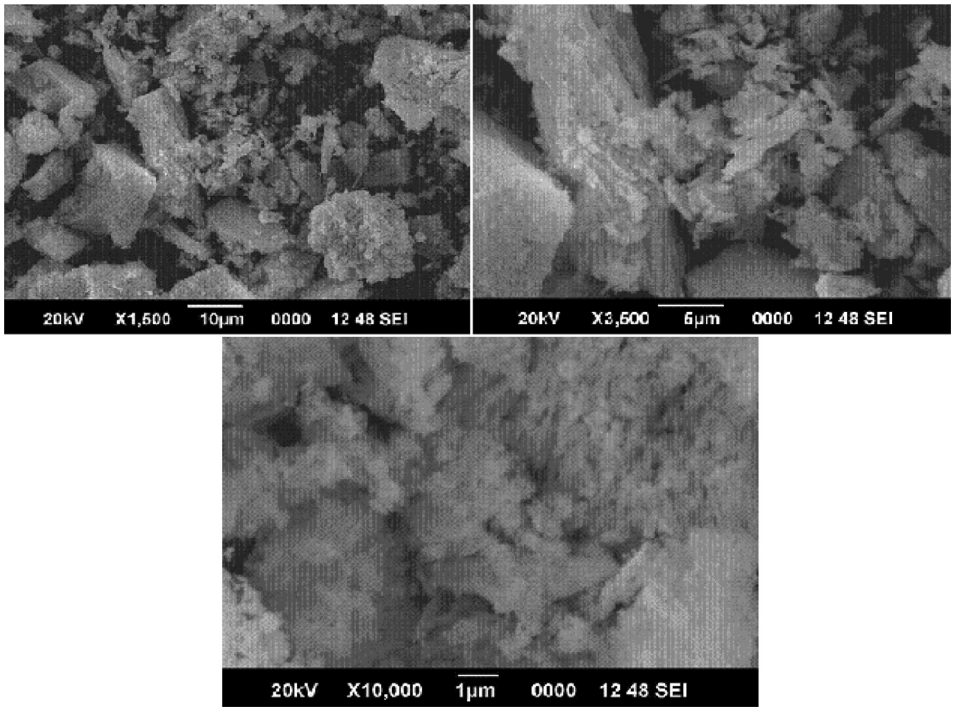

Fig. 15 SEM images of Nd_2O_3 residue of [Nd{2-$C_6H_4(CH_3CONH)COO\}_3.(N_2H_4)$].

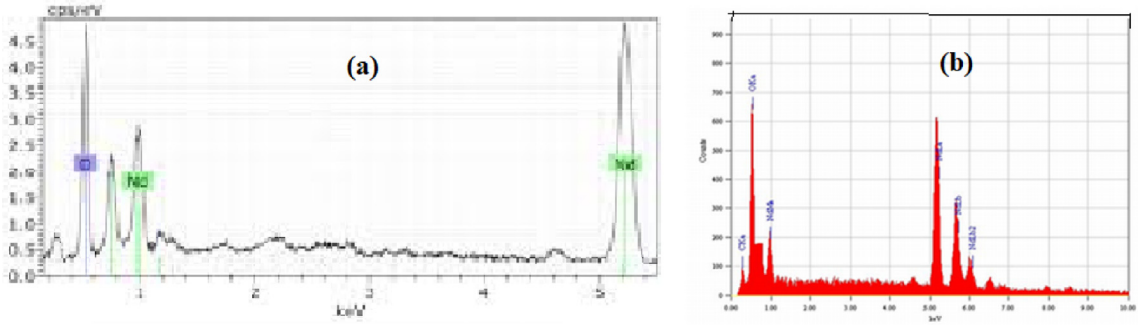

Fig. 16 SEM-EDAX image of (a) Nd_2O_3 nanoparticles (Reported); (b): Nd_2O_3 residue of $[Nd\{2\text{-}C_6H_4(CH_3CONH)COO\}_3.(N_2H_4)$.

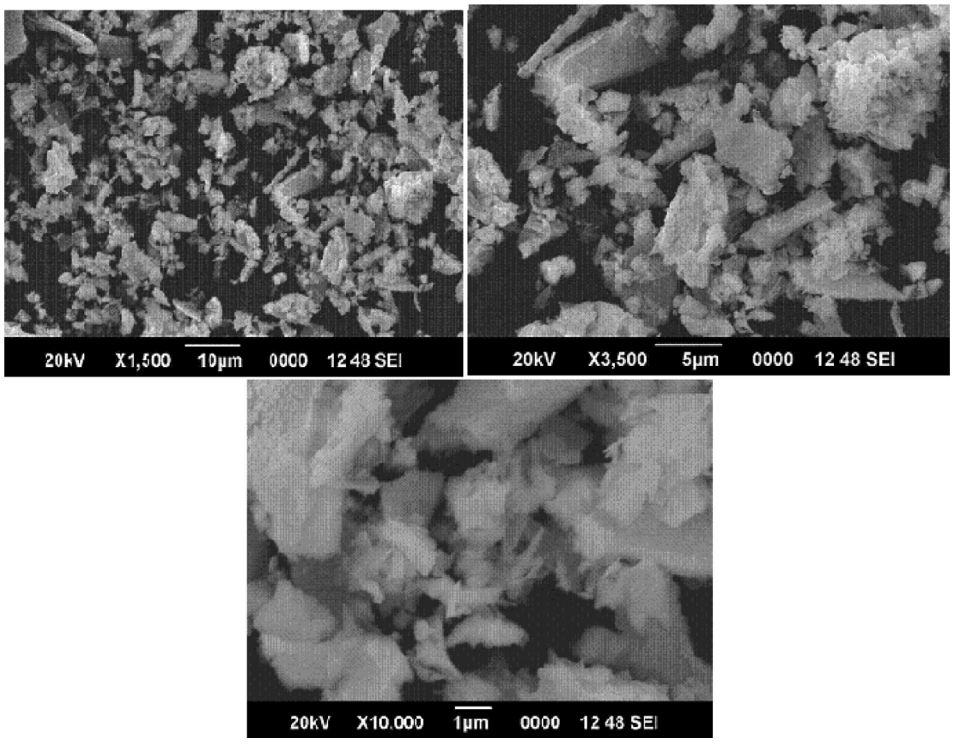

Fig. 17 SEM images of Pr_6O_{11} residue of $[Pr\{3\text{-}C_6H_4(CH_3CONH)COO\}_3.(N_2H_4)]$.

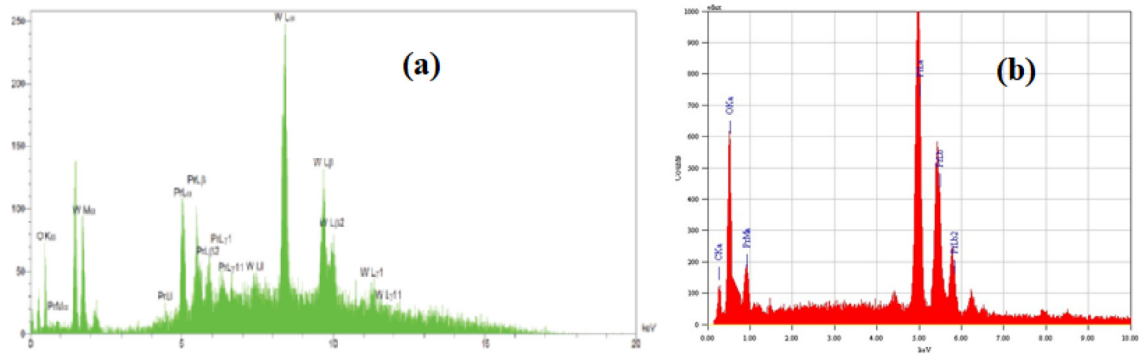

Fig. 18 SEM-EDAX image of (a)$Pr_2(WO_4)_3$Nanoparticles (reported; (b)Pr_6O_{11} residue of $[Pr\{3\text{-}C_6H_4(CH_3CONH)COO\}_3.(N_2H_4)]$.

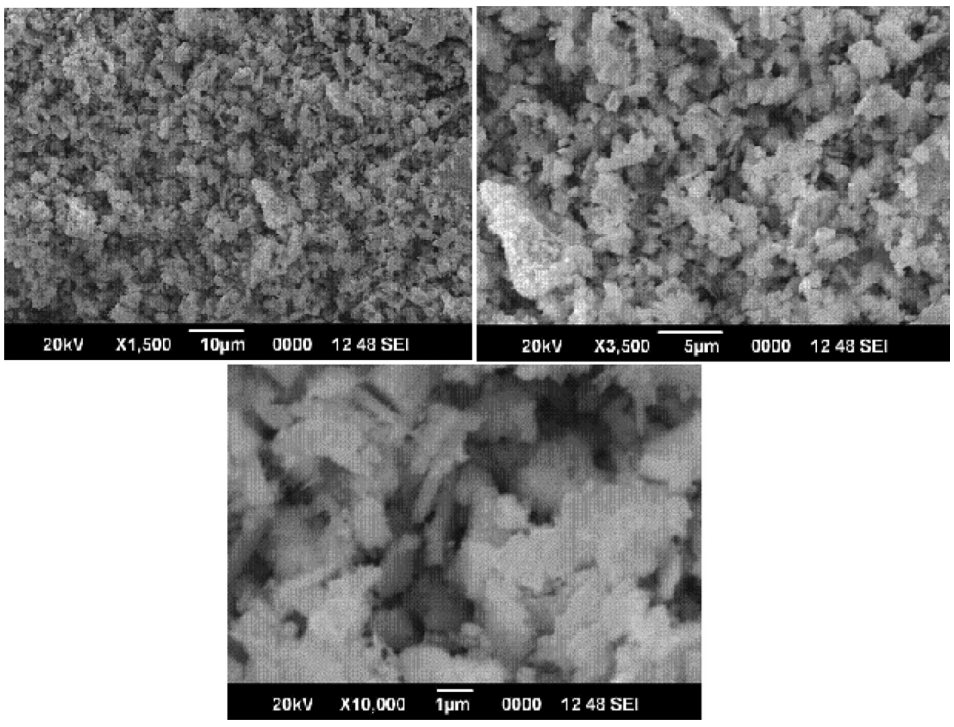

Fig. 19 SEM images of Pr_6O_{11} residue of[$Pr\{4\text{-}C_6H_4(CH_3CONH)COO\}_3(N_2H_4)$].

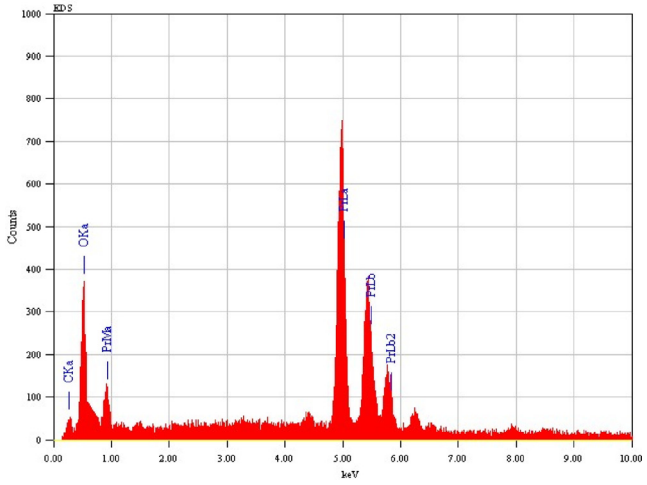

Fig. 20 SEM-EDAX image of Pr_6O_{11} residue.

plexes decompose to 1–10 µm sized metal oxides via metal phthalates intermediates as confirmed by their IR spectra, eliminating hydrazine below 200 °C. Cerium complexes decompose directly to their metal oxides via high unstable intermediates, showing difference in thermal behaviour. The NMR studies of the complexes substantiate the formation of complexes by showing the characteristic peaks of the acid moiety. The mass spectral data of the complex [$La\{x\text{-}C_6H_4(NHCOCH_3)COO\}_3(N_2H_4)$] where x = 2, 3 and 4, confirms the formation of the complex by showing the molecular ion peak. Based on the analytical and spectroscopic data, the structures of the complexes are proposed as depicted in the Fig. 24. The electronic spectral values indicate that the complexes may have coordination number 8. However, these structures can be confirmed by their single crystal analysis (see Fig. 25).

Declaration of Competing Interest

The authors declare that they have no known competing financial interests or personal relationships that could have appeared to influence the work reported in this paper.

Table 6 Molar Conductance of lanthanide complexes of isomeric acetamido benzoic acids and hydrazine.

S.No	Complexes	Specific Conductance (mmhos)	Molar Conductance (ohm^{-1} cm^2mol^{-1})
1	$[La\{2\text{-}C_6H_4(CH_3CONH)COO\}_3(N_2H_4)]$	0.30×10^{-3}	30
2	$[Pr\{2\text{-}C_6H_4(CH_3CONH)COO\}_3(N_2H_4)]$	0.24×10^{-3}	24
3	$[Gd\{2\text{-}C_6H_4(CH_3CONH)COO\}_3(N_2H_4)]$	0.1×10^{-3}	10
4	$[La\{4\text{-}C_6H_4(CH_3CONH)COO\}_3(N_2H_4)]$	0.13×10^{-3}	13
5	$[Ce\{4\text{-}C_6H_4(CH_3CONH)COO\}_3(N_2H_4)]$	0.12×10^{-3}	12
6	$[Gd\{4\text{-}C_6H_4(CH_3CONH)COO\}_3(N_2H_4)]$	0.08×10^{-3}	8

Table 7 Characteristic fragments of Mass spectrum of [La{C_6H_4 (CH_3CONH)COO}$_3$].

S. No.	Peak Value(m/z)	Fragmented Species (Ions & neutral)
1	59	CH_3CONH_2
2	121	$C_6H_5COO^-$
3	136	La^{3+}
4	166	$C_6H_4(COO)_2)^-$
5	303	$La\{C_6H_4(COO)_2)$
6	392 (Base Peak)	$(C_7H_5O_2)_3.N_2H_4$
7	707	[La{C_6H_4 (CH_3CONH)COO}$_3$]
8	1380	2[La{C_6H_4 (CH_3CONH)COO}$_3$.N_2H_4]

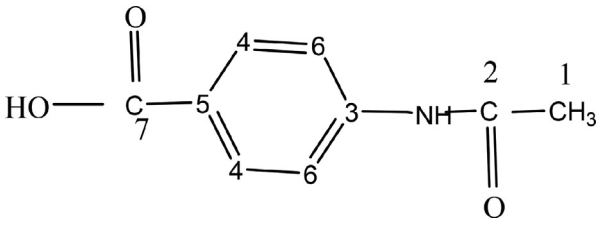

Fig. 21 4-acetamido benzoic acid with carbon numbering.

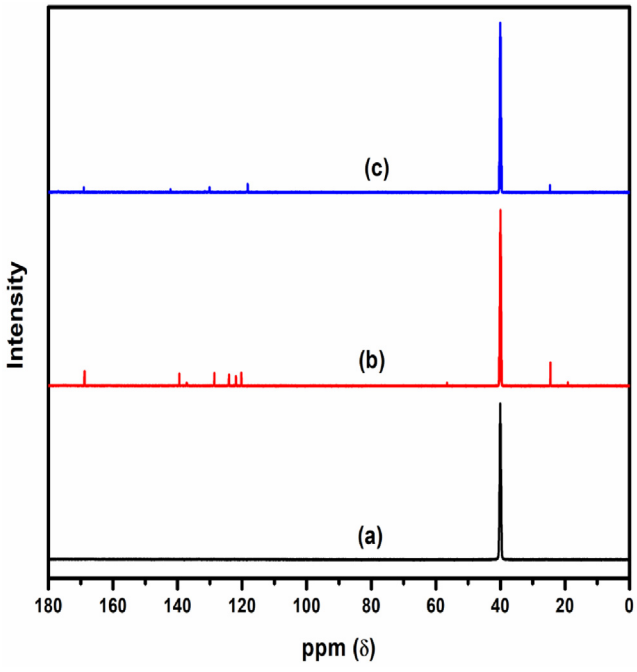

Fig. 22 ^{13}C – NMR Spectra of (a): [La{2-C_6H_4($NHCOCH_3$) COO}$_3$(N_2H_4)]; (b): [Gd{3-C_6H_4($NHCOCH_3$)COO}$_3$(N_2H_4)]; (c): [La{4-C_6H_4($NHCOCH_3$)COO}$_3$(N_2H_4)].

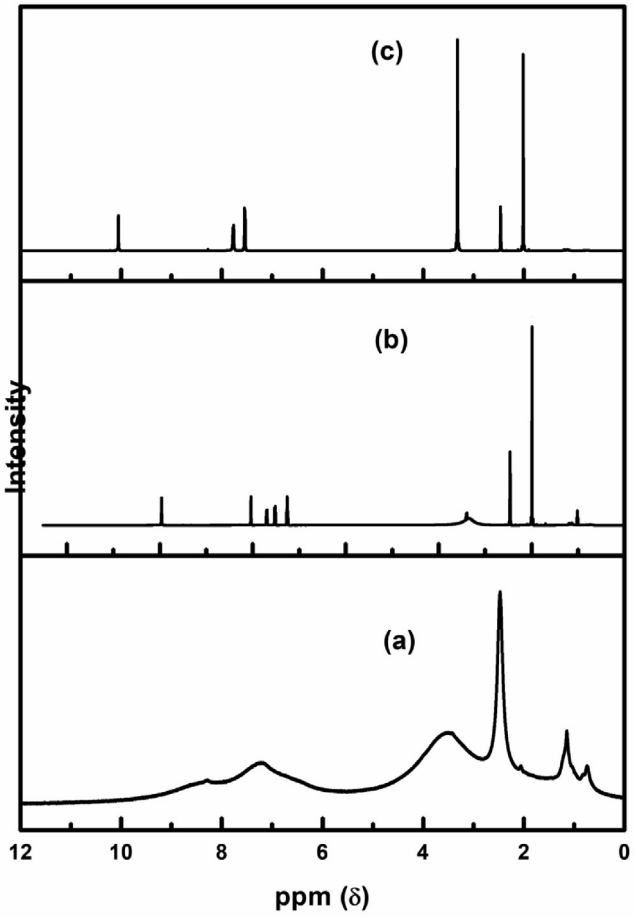

Fig. 23 ^{1}H – NMR Spectra of (a): [La{2-C_6H_4($NHCOCH_3$) COO}$_3$(N_2H_4)]; (b): [Gd{3-C_6H_4($NHCOCH_3$)COO}$_3$(N_2H_4)]; (c): [La{4-C_6H_4($NHCOCH_3$)COO}$_3$(N_2H_4)].

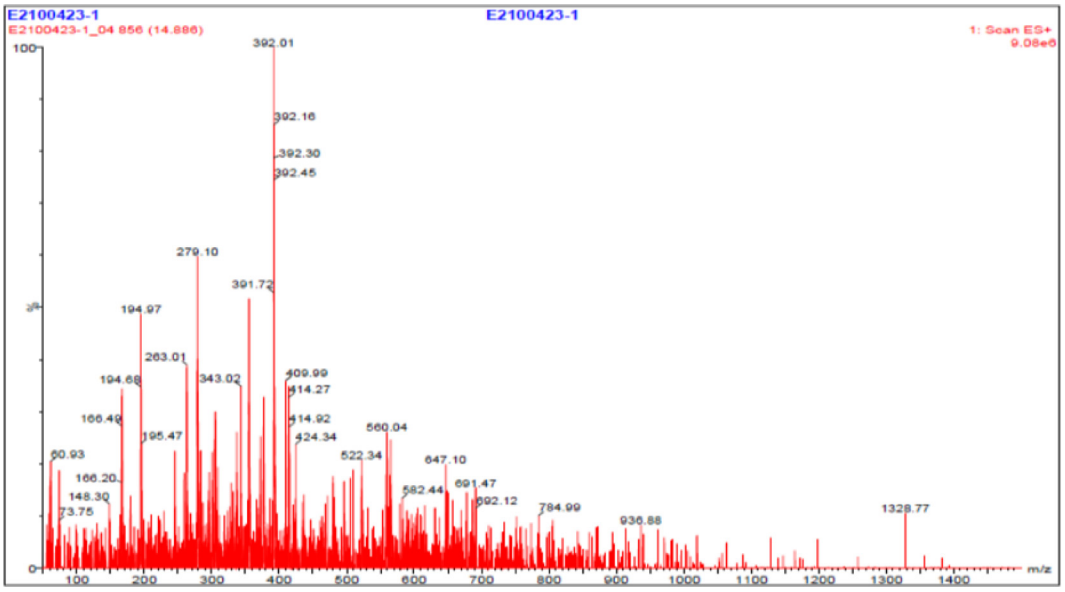

Fig. 24 Mass Spectrum of $[La\{C_6H_4(NHCOCH_3)COO\}_3(N_2H_4)]$.

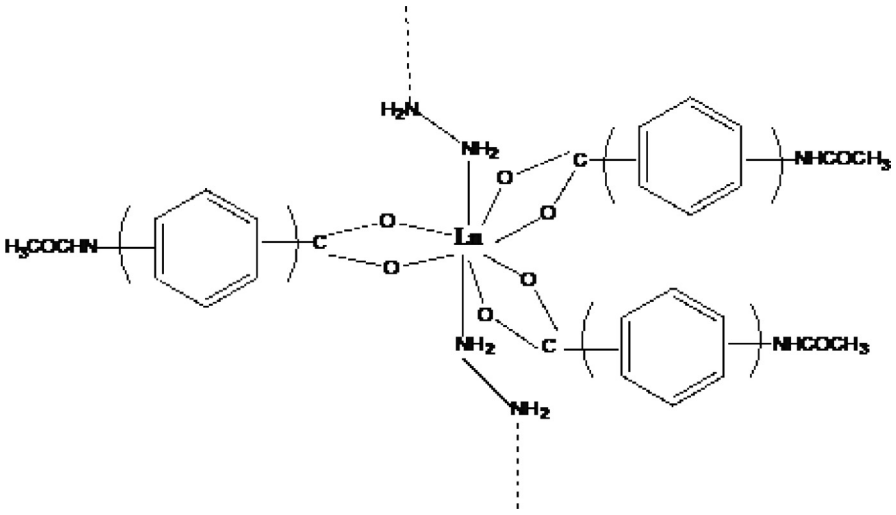

Fig. 25 Proposed structure of $[Ln\{2 / 3 \& 4\text{-}C_6H_4(CH_3CONH)COO\}_3(N_2H_4)]$ where Ln = La, Ce Pr, Nd, Sm& Gd.

Acknowledgment

The current research work was the grant-in-aid of All India council of Technical education, New Delhi, [8023/BOR/RID/RS, 2008- 2009]. The authors of the manuscript are thankful to the management and SITRA for helping in the successful completion of work.

References

Abraham, R.J., Loftus, P., 1980. Proton and carbon -13 NMR spectroscopy an integrated approach. Heyden & Son Ltd., London.

Almeida, A.R.R.P., Sousa, C.A.D., Santos, L.M.N.B.F., Monte, J.S., 2015. Thermodynamic properties of sublimation of the ortho and meta isomers of acetoxy and acetamido benzoic acids. J. Chem. Thermodyn. 86, 6–12.

Bai, E.H.P., Vairam, S., 2013a. Spectral and thermal studies of transition metal complexes of acetamido benzoic acids with hydrazine. Asian J. Chem. 25, 209–216.

Bai, E.H.P., Vairam, S., 2013b. Hydrazine complexes of Lanthanides with 3-acetoxy and 4-acetoxybenzoic acids: Spectroscopic, thermal and XRD studies. J. Chem. 2013, 1–10.

Bai, E.H.P., Vairam, S., 2020. A Study on Thermal Degradation of hydrazinated transition metal acetamido benzoates. Current perspectives on chemical sciences, 1st edition, India &UK. 2, 90–106.

Berryman, V.E.J., Whalley, Z.J., Shephard, J.J., Ochiai, T., Price, A. N., Arnold, P.L., Parsons, S., Kaltsoyannis, N., 2019. Computational analysis of M-O covalency in $M(OC_6H_5)_4$ (M = Ti, Zr, Hf, Ce, Th, U). Dalton Trans. 48, 2939–2947.

Braibanti, A., Dallavalle, F., Pellinghelli, M.A., Leporati, E., 1968. The nitrogen-nitrogen stretching band in hydrazine derivatives and complexes. Inorg. Chem. 7, 1430–1433.

Devipriya, S., Arunadevi, N., Vairam, S., 2013. Synthesis and Thermal Characterization of Lanthanide(III) Complexes with Mercaptosuccinic Acid and Hydrazine as Ligands. J. Chem. 2013, 1–10.

Gaye, M., Tamboura, F.B., Sall, A.S., 2003. Spectroscopic studies of some lanthanide (III) nitrate complexes synthesized from a new ligand 2,6-bis-(salicylaldehyde hydrazone)-4-chlorophenol. Bull. Chem. Soc. Ethiop. 17, 27–34.

Geary, W.J., 1971. The use of conductivity measurements in organic solvents for the characterization of coordination compounds. Coord. Chem. Rev. 7, 81–122.

Gorgola, R.K., Brzyska, W., 1999. Preparation and properties of rare earth 4-nitrophthalates. Croat. Chem. Acta. 72, 77–86.

Govindarajan, S., Patil, K.C., Manohar, H., Werner, P.E., 1986. Hydrazinium as a ligand – structural, thermal, spectroscopic, and magnetic studies of hydrazinium lanthanide di-sulfate monohydrates – crystal structure of the neodymium compound. J. Chem. Dalton Trans. 1, 119–123.

Gupta, M.K., 2019. Synthesis, antimicrobial evaluation and docking studies of novel 4-acetamido-3-aminobenzoic acid derivatives as microbial neuraminidase inhibitors. Research J. Pharm. and Tech. 12, 303–313.

Jung, J., Atanasov, M., Neese, F., 2017. Ab initio ligand-field theory analysis and covalency trends in actinide and lanthanide free ions and octahedral complexes. Inorg. Chem. 56, 8802–8816.

Kuppusamy, K., Sivasankar, B.N., Govindarajan, S., 1996. Preparation and thermal reactivity of hydrazinium uranyl carboxylates. Thermochim. Acta. 274, 139–148.

Lembang, M.S., Yulizar, Y., Sudirman, S., Apriandanu, D.O.B., 2018. A facile method for green synthesis of Nd_2O_3 nanoparticles using aqueous extract of terminalia catappa leaf. AIP Conf. Proc. 020093, 1–6.

Li, W., Li, C.-H., Yang, Y.-Q., Kuang, Y.-F., 2007. Hydrothermal synthesis, crystal structure and thermal stability of the complex [Zn (p-ABA)2(phen0. ($_H$2O)].$_H$2O. Chinese J. Inorg. Chem. 23, 2023–2027.

Man, B.Y.W., 2010. Transition Metal and Lanthanide Complexes for Catalysis and Protein Structure Determination PhD Thesis, submitted to. The University of New South Wales School of Chemistry.

Manin, A.N., Voronin, A.P., Drozd, K.V., Manin, N.G., Bauer-Brandl, A., Perlovich, G.L., 2014a. Cocrystal screening of hydroxybenzamides with benzoic acid derivatives: a comparative study of thermal and solution-based methods. Eur. J. Pharm. Sci. 65, 56–64.

Manin, A.N., Voronin, A.P., Manin, N.G., Vener, M.V., Shishkina, A.V., Lermontov, A.S., Perlovich, G.L., 2014. Salicylamide Cocrystals: Screening, Crystal Structure, Sublimation Thermodynamics, Dissolution, and Solid-State DFT Calculations. J. Phys. Chem. B 118, 6803–6814.

Manin, A.N., Voronin, A.P., Perlovich, G.L., 2014b. Acetamidobenzoic acid isomers: Studying sublimation and fusion processes and their relation with crystal structures. Thermochim. Acta. 583, 72–77.

Mascarenhas, Y.P., de Almeida, V.N., Lechat, J.R., Barelli, N., 1980. N-Acetylanthranilic acid (O-acetamidobenzoic acid) a strongly triboluminescent material. Acta. Crystallogr. B. Struct. Sci. Cryst. Eng. Mater. 36, 502–504.

Milenkovic, M., Warzajtis, B., Urszula, R., Dusanka, R., Katarina, A., Tatjana, B., Miroslava, V., 2012. Synthesis, Spectral and solid-State Characterization of a new Bioactive Hydrazine bridged Cyclic Diphosphonium Compound. Molecules. 17, 2567–2578.

Nakamoto, K. et al, 2009. Infrared and Raman Spectra of Inorganic and Co-ordination Compounds, 6thedition. Wiley Interscience Co, New York, USA.

Parimalagandhi, K., Premkumar, T., Vairam, S., 2016. A general method for preparing lanthanide oxide nanoparticles via thermal decomposition of lanthanide(III) complexes with 1-hydroxy-2-naphthoic acid and hydrazine ligands. J. Phys. Chem. Solids 96, 60–67.

Parimalagandhi, K., Vairam, S., 2014. Kinetics and thermal decomposition of Tetrahydrazine lanthanum 2-hydroxy-1- naphthoate. Orient. J. Chem. 30, 1957–1963.

Pavia, L., Lampman, G.M., krizand, G.A., Vyvyan, J.R., 2015. Introduction to spectroscopy, 5th edition, Cengage Learning, USA.

Petit, L., Borel, A., Daul, C., Maldivi, P., Adamo, C., 2006. A theoretical characterization of covalency in rare earth complexes through their absorption electronic properties:f-f transition. Inorg. Chem. 45, 7382–7388.

Pourmortazavi, S.M., Rahimi-Nasrabadi, M., Ganjali, M.R., Karimi, M.S., Norouzi, P., Faridbod, F., 2017. Facile and effective synthesis of praseodymium tungstate nanoparticles through an optimized procedure and investigation of photocatalytic activity. Open Chem. 15, 129–138.

Rakse, M., Karthikeyan, C., Moorthy, N.S.H.N., Agrawal, K.R., 2021. Design, Synthesis and Biological Evaluation of 3-(2-(benzo[d] thiazol-2- ylthio)acetamido)benzoic Acid Derivatives as Inhibitors of Protein Tyrosine Phosphatase 1B. Lett. Drug Des. Discov. 18, 46–56.

Ramalingam, S.K., Soundararajan, S., 1967. Dimethyl sulphoxide complexes of lanthanide and yttrium nitrates. J. Inorg. Nucl. Chem. 29, 1763–1768.

Ravindranathan, P., Mahesh, G.V., Patil, K.C., 1987. Low-temperature preparation of fine-particle cobaltites. J. Solid State Chem. 66, 20–25.

Ravindranathan, P., Patil, K.C., 1986. A one-step process for the preparation of γ-Fe_2O_3. J. Mat. Sci. Lett. 5, 221–222.

Schmidt, E.W. et al, 1984. Hydrazine and its Derivatives - Preparation, Properties and Applications. Wiley Inter. Sci., NY, USA.

Sivasankar, B.N., Sharmila, J.R., Saratha, R., Govindarajan, S., 2004. Preparation and thermal reactivity of some rare earth and uranyl hydrazine sulfinates and sulfite hydrazinates. Thermochim. Acta. 417, 107–113.

TanTong, J., Xu, T., Liu, S., Zhang, J., Hou, X., Liu, B., 2018. Cascade covalent and coordination bond formation for Ti-based cage assembly: catalysis and coordination bifunctionality of $TiCl_4$. Dalton Trans. 47, 3239–3242.

Vairam, S., Govindarajan, S., 2006. Hydrazinium complexes of Lanthanide and Transition metal squarates. Polish J. Chem. 80, 1601–1614.

Vogel, A.I., 2019. A Text Book of Quantitative Inorganic Analysis Including Elemental Analysis. Longmans, London, UK.

Wang, Z.-H., Fan, J., Zhang, W.-G., 2009. Studies of radii-dependent lanthanide coordination behavior with 4-acetamidobenzoate and 1,10-phenanthroline. Z. Anorg. Allg. Chem. 635, 2333–2339.

Want, B., Shah, M.D., 2016. Magnetic susceptibility measurements of pure and mixed gadolinium-terbium formate heptahydrate crystals. J. Magn. Magn. Mater. 401, 391–393.

Yang, Y.-Q., Li, C.-H., Li, W., Kuang, Y.-F., 2009. Solvothermal Synthesis, Crystal Structure and Electrochemical Properties of the Complex Cd-2(2,4-DAA)(4)(phen)(2). Chinese J. Inorg. Chem. 25, 1120–1123.

Yang, Y.-Q., Li, C.-H., Li, W., Yi, Z.-J., 2009a. Synthesis, crystal structure and fluorescence characterization of cadmium(II) coordination polymer with 4-acetamidobenzoic acid and 4, 4'-bipyridine. Chinese J. Inorg. Chem. 25, 1304–1307.

Yin, X., Fan, J., Wang, Z., Zhang, W.-G., 2011. Synthesis, crystal structures, and photoluminescence of Lanthanide coordination polymers with 4-acetamidobenzoate. Z. Anorg. Allg. Chem. 637, 773–777.

Zoubi, W.A., Nashrah, N., Chaouiki, A., GunKo, 2021. Self-assembled molecular network formed by controlling molecular deposition of organic compounds. Flat Chem. 29.

Zoubi, W.A., Kamil, M.P., Fathima, Nashrah, N., Ko, Y.G., 2020. Recent advances in hybrid organic-inorganic materials with spatial architecture for state-of-the-art applications. Prog. Mat. Sci. 112.